



**British
Geological Survey**

NATURAL ENVIRONMENT RESEARCH COUNCIL

The development and validation of the object-oriented quasi three- dimensional regional groundwater model ZOOMQ3D

Groundwater Systems and Water Quality

Internal Report IR/01/144

BRITISH GEOLOGICAL SURVEY

INTERNAL REPORT IR/01/144

The development and validation of the object-oriented quasi three- dimensional regional groundwater model ZOOMQ3D

C.R. Jackson

The National Grid and other
Ordnance Survey data are used
with the permission of the
Controller of Her Majesty's
Stationery Office.
Ordnance Survey licence number
GD 272191/1999

Bibliographical reference

JACKSON C.R., 2001. The
development and validation of
the object-oriented quasi three-
dimensional regional
groundwater model ZOOMQ3D.
*British Geological Survey
Internal Report, IR/01/144.*
57pp.

BRITISH GEOLOGICAL SURVEY

The full range of Survey publications is available from the BGS Sales Desks at Nottingham and Edinburgh; see contact details below or shop online at www.thebgs.co.uk

The London Information Office maintains a reference collection of BGS publications including maps for consultation.

The Survey publishes an annual catalogue of its maps and other publications; this catalogue is available from any of the BGS Sales Desks.

The British Geological Survey carries out the geological survey of Great Britain and Northern Ireland (the latter as an agency service for the government of Northern Ireland), and of the surrounding continental shelf, as well as its basic research projects. It also undertakes programmes of British technical aid in geology in developing countries as arranged by the Department for International Development and other agencies.

The British Geological Survey is a component body of the Natural Environment Research Council.

Keyworth, Nottingham NG12 5GG

☎ 0115-936 3241 Fax 0115-936 3488
e-mail: sales@bgs.ac.uk
www.bgs.ac.uk
Shop online at: www.thebgs.co.uk

Murchison House, West Mains Road, Edinburgh EH9 3LA

☎ 0131-667 1000 Fax 0131-668 2683
e-mail: scotsales@bgs.ac.uk

London Information Office at the Natural History Museum (Earth Galleries), Exhibition Road, South Kensington, London SW7 2DE

☎ 020-7589 4090 Fax 020-7584 8270
☎ 020-7942 5344/45 email: bgs london@bgs.ac.uk

Forde House, Park Five Business Centre, Harrier Way, Sowton, Exeter, Devon EX2 7HU

☎ 01392-445271 Fax 01392-445371

Geological Survey of Northern Ireland, 20 College Gardens, Belfast BT9 6BS

☎ 028-9066 6595 Fax 028-9066 2835

Macleans Building, Crowmarsh Gifford, Wallingford, Oxfordshire OX10 8BB

☎ 01491-838800 Fax 01491-692345

Parent Body

Natural Environment Research Council, Polaris House, North Star Avenue, Swindon, Wiltshire SN2 1EU

☎ 01793-411500 Fax 01793-411501
www.nerc.ac.uk

Contents

Contents	i
Acknowledgements	1
Summary	1
1 Introduction	1
2 Simulating unconfined conditions	2
2.1 Representation of unconfined conditions in ZOOMQ3D	2
2.2 Validation of unconfined behaviour	6
3 Layers	12
3.1 Representation of layers in ZOOMQ3D	12
3.2 One dimensional vertical flow problem.....	13
3.3 Comparison with the model of Szekely (1998)	15
4 Springs	21
5 Moving boundaries: node de-watering and re-wetting	22
5.1 Background	22
5.2 1D steady state flow in an unconfined aquifer.....	22
5.3 Vertical slice through a multi-layered aquifer	23
5.4 Moving boundary in a sloping bed aquifer	30
6 Anisotropy	33
6.1 The validation test problem	33
6.2 The MODFLOW model.....	33
6.3 ZOOMQ3D Model 1 – regular 27.5 m mesh model.....	34
6.4 ZOOMQ3D Model 2 – locally refined mesh.....	36
6.5 ZOOMQ3D Model 3 – locally refined mesh.....	38
7 Numerical solvers	39
8 The simulation of ephemeral rivers	39
8.1 Background.....	39
8.2 The influence of groundwater abstraction on river flow	40
8.3 Sloping river model with sinusoidally varying recharge	42
8.4 Oakes and Wilkinson analytical solution to time variant flow in a perennial river.....	44
9 Concluding remarks	49
10 References	50

FIGURES

Figure 1	Use of inheritance to define confined and unconfined aquifer conditions	3
Figure 2	Example of specification of nodes by different types	4
Figure 3	Flowchart of the cyclical transmissivity updating process when simulating unconfined aquifers	5
Figure 4	Refined grid used to simulate 1-D unconfined aquifer	7
Figure 5	Steady state groundwater head profiles for 1-D model	7
Figure 6	Groundwater hydrographs on western boundary for 1-D models showing progress towards steady state solution	8
Figure 7	Refined grid model	9
Figure 8	Simulated groundwater head at the pumped well and at the position of the edge of the refined grid by both models	10
Figure 9	Groundwater head profiles at the end of the two-year simulation period	11
Figure 10	Calculation of the vertical conductance between layers in ZOOMQ3D	12
Figure 11	Drawdowns simulated by MODFLOW and ZOOMQ3D 1-D flow models	14
Figure 12	Node-centred grid of Szekely (1998)	15
Figure 13	Schematic of the iterative solution procedure of Szekely (1998)	16
Figure 14	Model mesh of Szekely (1998)	17
Figure 15	Steady state groundwater head contours after Szekely (1998)	19
Figure 16	Steady state groundwater head contours computed by ZOOMQ3D	20
Figure 17	Simulated heads and analytical solution for 1-D flow in unconfined aquifer	22
Figure 18	Multi-layer MODFLOW model presented by Anderson (1993)	23
Figure 19	Comparison between MODFLOW and ZOOMQ3D simulated heads	27
Figure 20	1-D Sloping bed model of unconfined/confined aquifer	31
Figure 21	Groundwater hydrographs for unconfined sloping bed model	32
Figure 22	Simulated spring flows in the unconfined sloping bed model	32
Figure 23	Comparison of 27.5 m square mesh ZOOMQ3D model with analytical solution and MODFLOW model	34
Figure 24	Groundwater head contours at the end of the one-day pumping test simulated by a) the MODFLOW model of Anderson (1993) and b) ZOOMQ3D	35
Figure 25	Locally refined grid ZOOMQ3D Model 2 to simulate anisotropic aquifer	36
Figure 26	Comparison of refined grid ZOOMQ3D model with analytical solution and MODFLOW model	37
Figure 27	Locally refined grid ZOOMQ3D Model 3 to simulate anisotropic aquifer	38
Figure 28	Model configuration for river/groundwater abstraction test problem	40
Figure 29	Nodal river flow hydrographs	41
Figure 30	Observed groundwater heads at nodes beneath river	41
Figure 31	Simulated river flows in sloping bed aquifer at dynamic balance	43

Figure 32	MODFLOW model after Prudic (1989)	45
Figure 33	Annual recharge pattern after Prudic (1989)	45
Figure 34	ZOOMQ3D model grid for comparison with the MODFLOW model of Prudic (1989) and the analytical solution of Oakes and Wilkinson (1972)	46
Figure 35	Computed head at the observation well by the a) the MODFLOW model of Prudic (1989) and the analytical solution b) the ZOOMQ3D model	47
Figure 36	Computed downstream river flow by the a) the MODFLOW model of Prudic (1989) and the analytical solution b) the ZOOMQ3D model	48

TABLES

Table 1	Vertical conductances for 1-D vertical flow model	13
Table 2	Drawdowns simulated by MODFLOW and ZOOMQ3D 1-D flow models	14
Table 3	Parameters for model presented by Szekely (1998)	17
Table 4	Comparison between analytical solution and Szekely and ZOOMQ3D models	18
Table 5	Specified heads in layer six of multi-layer MODFLOW model	25
Table 6	Parameter values for the six-layer MODFLOW model	26
Table 7	Monthly recharge rates (mm/day) for sloping bed model	31
Table 8	Model parameters for anisotropic aquifer test problem	33
Table 9	Grid spacing of MODFLOW model of anisotropic aquifer	33
Table 10	Nodal river flows and groundwater heads beneath the river	42
Table 11	Monthly recharge rates for model of sloping river	42
Table 12	High and low river flows in sloping river at dynamic balance	43
Table 13	Daily recharge rates calculated from Figure 33	44

Acknowledgements

This work has been undertaken as part of a continuing tripartite collaboration between BGS, Dr A Spink of The University of Birmingham and P Hulme and S Fletcher of the Environment Agency based at the National Groundwater and Contaminated Land Centre.

Summary

This report documents the modifications made to the object-oriented regional groundwater model ZOOM2D (The University of Birmingham, 2001). Additional mechanisms are introduced to this model to satisfy the generally-accepted functional requirements of a commonly-applied regional groundwater flow model. The modified model, ZOOMQ3D, is quasi three-dimensional and is validated through comparison with analytical solutions and with instructional problems formulated for MODFLOW (McDonald and Harbaugh, 1988) by Anderson (1993).

1 Introduction

The quasi three-dimensional model ZOOMQ3D is based on the earlier model ZOOM2D, developed by the University of Birmingham (2001), which incorporates local grid refinement (Jackson, 2000). ZOOM2D is a two-dimensional regional groundwater flow model based on the governing groundwater flow equation (Bear, 1979) of the form:

$$\frac{\partial}{\partial x} \left(T_x \frac{\partial h}{\partial x} \right) + \frac{\partial}{\partial y} \left(T_y \frac{\partial h}{\partial y} \right) = S \frac{\partial h}{\partial t} - q$$

Aquifer properties are allowed to vary in space but are constant in time. Therefore, the model will be accurate in confined aquifers or in unconfined aquifers where groundwater head variations are small compared to the saturated thickness. In addition to the local grid refinement algorithm the model includes other typical features required to simulate regional groundwater flow. Dendritic river basins made up of multiple river reaches, groundwater abstraction and injection wells and variable aquifer recharge are included. Interactions between the aquifer and surface water features are implemented as linear leakage mechanisms.

Whilst ZOOM2D is a usable model for the simulation of many regional aquifers it does not incorporate some of the mechanisms that are commonly required by hydrogeological modellers. Consequently, ZOOM2D has been developed further to include the required mechanisms. The resulting code is called ZOOMQ3D. The mechanisms added to ZOOM2D in ZOOMQ3D are:

- The ability to represent unconfined conditions based on the variation of transmissivity with saturated thickness.
- The inclusion of layers to represent different hydrogeological strata.
- The de-watering and re-wetting of model nodes to allow for the simulation of moving boundaries.
- The simulation of springs.
- Horizontal anisotropy.

In addition to these newly introduced mechanisms three limitations of ZOOM2D have been addressed. They are:

- The creation of ‘magic’ water along a river as reaches dry up.
- The use of a single conductance parameter by head dependent leakage nodes when they are both influent and effluent.
- The rewriting of solver objects for clarity and flexibility.

A description of these bulleted points is given in each of the following sections. Where appropriate the validation of the model changes is described.

One of the aims of this development work is to provide the modelling community with a model with which to assess the benefits of the object-oriented approach to groundwater modelling. However, the project partners view the current model as a *step* towards the development of the final object-oriented regional groundwater model that better represents UK hydrogeology.

The object-oriented paradigm is a relatively new and powerful approach for developing software. In particular it offers significant benefits to the accurate representation of physical mechanisms in models. It can also greatly simplify the maintenance and development of a model as the understanding of the physics of groundwater flow improves. This is because real world objects are modelled by computational equivalents. The objects may incorporate complex processes but it is only necessary to represent their interactions. This separation of concerns not only simplifies the program structure but, more importantly, allows better descriptions of physical processes within the model.

The further development of the object-oriented regional groundwater model, ZOOMQ3D, is described in the following sections. Each section deals with the incorporation or updating of an individual component of the model and its validation. In Section 2 the representation of unconfined aquifers is discussed. In Section 3 the incorporation of layers in the model is described. In general the use of layers increases the likelihood that one of the nodes of the grid will de-water. Springs are often simulated in groundwater models using head dependent leakage nodes, the flow from which is calibrated by adjusting its conductance parameter. An additional mechanism is added to simulate springs which is not based on a conductance term. This is described in Section 4. The method by which nodes are allowed to de-water and re-wet and its validation is described in Section 5. The ability to define anisotropy at each node is implemented in the model and this is discussed in Section 6. In the final two sections two aspects of the previous model are improved. In Section 7 an improved implementation of numerical solution algorithms within the model is described and in Section 8 the technique for the simulation of ephemeral rivers is modified and validated. In some of the validation tests described subsequently, model parameter values are given to an apparently large number of decimal places. Where this is the case, it is because they have been quoted to this level of accuracy in the literature on which the tests are based.

2 Simulating unconfined conditions

2.1 REPRESENTATION OF UNCONFINED CONDITIONS IN ZOOMQ3D

Unconfined behaviour is incorporated in the model using the object-oriented concept of *inheritance*. Three types of node objects are defined in the object framework: CNode, CConfinedNode and CConvertibleNode. The objects of type CConfinedNode and CConvertibleNode are derived from the base class CNode. Objects are never created directly from the CNode class. Instead, only objects of type CConfinedNode and CConvertibleNode are created.

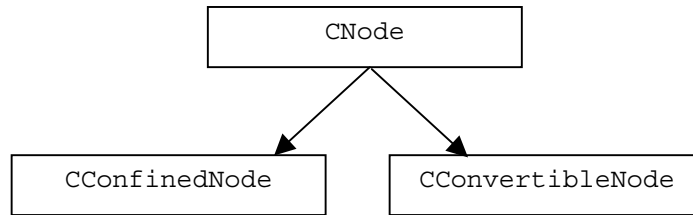


Figure 1 Use of inheritance to define confined and unconfined aquifer conditions

In CConfinedNode objects the transmissivity is always constant as it is independent of the groundwater head. CConvertibleNode objects contain the functionality to calculate transmissivity based on the difference between the groundwater head and the elevation of the base of the node. This is a linear relationship as the horizontal hydraulic conductivity is assumed to be uniform in the vertical direction:

$$T = K \cdot (h - z_B)$$

Transmissivity is limited to a maximum value when the groundwater head rises above the top of the node. The maximum transmissivity is given by:

$$T = K \cdot (z_T - z_B)$$

where:

- h is the groundwater head
- T is the transmissivity
- K is the horizontal hydraulic conductivity
- z_T is the elevation of the top of the node
- z_B is the elevation of the base of the node

In Section 5 the addition of layers to the model is described. In the top layer of the model, nodes are defined to be either:

- i. always confined (c),
- ii. always unconfined (u). These nodes are only allowed in the top layer,
- iii. or convertible (v) i.e. to switch between unconfined and confined conditions

Currently all nodes must be of the same type in each lower layer as is the case in MODFLOW. Additionally, in the lower layers nodes can only be confined (c) or convertible (v). CConvertibleNode objects represent both of the cases ii) and iii) listed above. A character member variable of the CConvertibleNode class defines if the node is unconfined or if it is convertible. The transmissivity is not limited by the upper elevation of the node if it is unconfined.

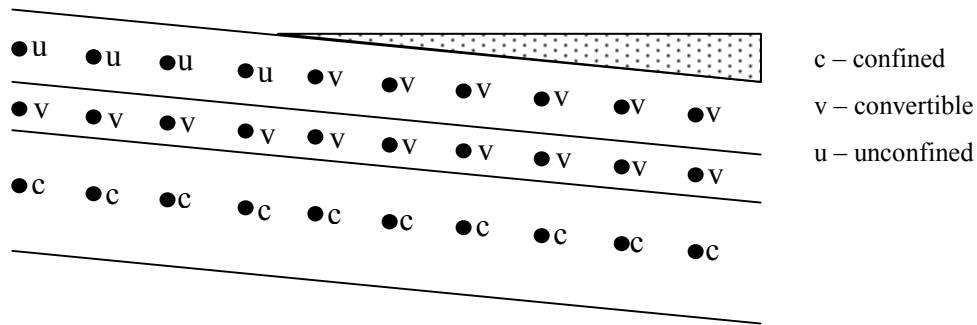


Figure 2 Example of specification of nodes by different types

Unconfined behaviour is represented as a cyclical process within the model. The finite difference equations are solved repeatedly during *each* time step. Each unconfined node calculates its transmissivity at the beginning of the time step based on the groundwater head. A solution to the finite difference equations is then computed. The transmissivity is subsequently recalculated using the new heads. An average is then taken of the pre and post-solution transmissivities at each unconfined node. A new solution to the finite difference equations is computed again using the average of the two transmissivity values. This cyclical process continues until the transmissivity variation over a cycle is negligible at all the unconfined nodes.

The test for convergence within the repetitive cycle is based on a maximum nodal flow imbalance. At the end of a cycle, after the solution has been computed and the averages of the transmissivities have been calculated, nodal flow imbalances are examined. Nodal flow balances are calculated using the heads computed at the end of the i^{th} cycle (based on the transmissivities at the beginning of the i^{th} cycle) and the average transmissivities calculated at the end of the i^{th} cycle. If the maximum flow imbalance is below a small user defined value then the difference between the pre and post solution transmissivities is small. The solution then progresses to the *next* time step. This process is illustrated in Figure 3.

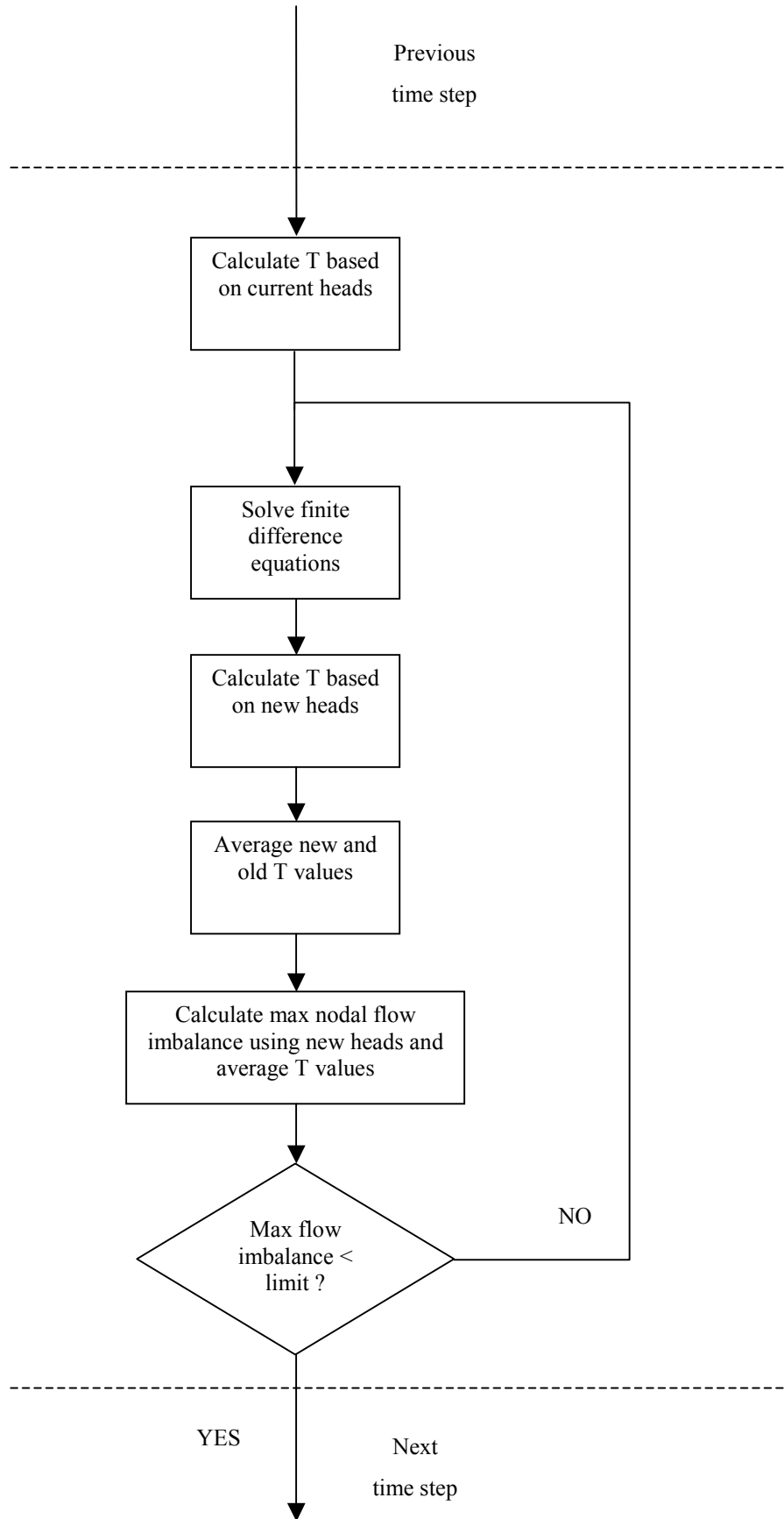


Figure 3 Flowchart of the cyclical transmissivity updating process when simulating unconfined aquifers

2.2 VALIDATION OF UNCONFINED BEHAVIOUR

The simulation of unconfined aquifers by ZOOMQ3D is validated using two tests. The first is a comparison with an analytical solution to a one-dimensional steady state problem. The second test examines whether local grid refinement remains applicable when simulating phreatic aquifers. This is found to be the case.

2.2.1 Analytical solution to one-dimensional steady state flow in an unconfined aquifer

The aquifer simulated is 10 km long from west to east. The western boundary is impermeable and the eastern boundary is specified as a constant head boundary with heads fixed at 100 m above the base of the aquifer. The aquifer is unconfined and receives recharge uniformly at a rate of 1 mm/day. It is homogenous with a hydraulic conductivity of 10 m/day and a specific yield of 0.01. The model contains a single layer.

The analytical solution to this one-dimensional steady state problem is:

$$h^2 = \frac{q}{K}(L^2 - x^2) + H^2$$

where: h is the groundwater head (m),
 q is the recharge rate (m/day),
 K is the hydraulic conductivity (m/day),
 L is the length of the aquifer (m),
 x is the distance from the western boundary (m) and
 H is the groundwater head specified on the eastern boundary (m).

The aquifer is simulated using three different finite difference grids, which are all 10 km square. The first two are based on uniform regular square meshes of 1 km and 250 m. The third is shown in Figure 4 and has been refined in the centre of the model domain. The base grid is composed of 1 km square cells. These are refined in the central 4 km square region to 250 m square cells. All model boundaries are impermeable except for the right hand, or eastern boundary, which is the constant head boundary.

The steady state solution is computed by simulating a ten-year period of constant recharge. Initially groundwater heads are all 100 m above the base of the aquifer. The comparison between the simulated steady state groundwater head profile and the analytical solution is shown in Figure 5. These are in good agreement and the maximum difference in head is less than 4 cm. The groundwater heads are monitored on the western boundary during the simulations. These groundwater hydrographs are shown in Figure 6 and indicate that the temporal variation in transmissivity is similar for each model.

The same nodal flow balance convergence criterion of 10^{-8} m³/day is used for each of the three models. The regular 1 km grid model simulations takes 23 seconds to run and the regular 250 m grid model takes 12.5 minutes to converge. The refined grid model converges after 90 seconds and is therefore approximately 85 times faster than the regular fine grid model. However, the refined grid model is slightly less accurate than the regular grid models. This is because the finite difference approximations on the edge of the refined mesh are slightly less accurate than those on a regular mesh when transmissivity is non-uniform across the parent-child grid boundary. A full description of this phenomenon is presented by Jackson (2000).

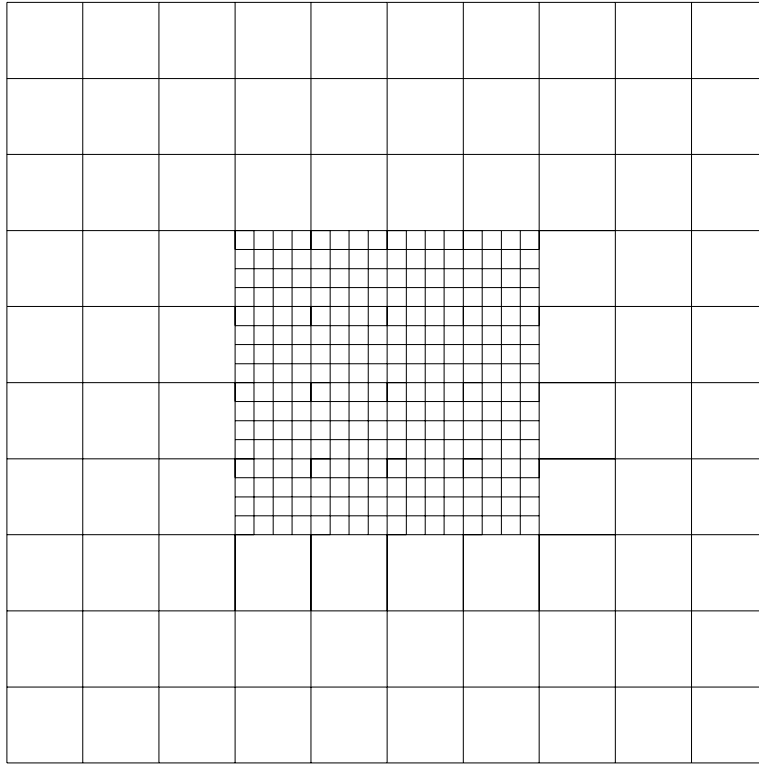


Figure 4 Refined grid used to simulate 1-D unconfined aquifer

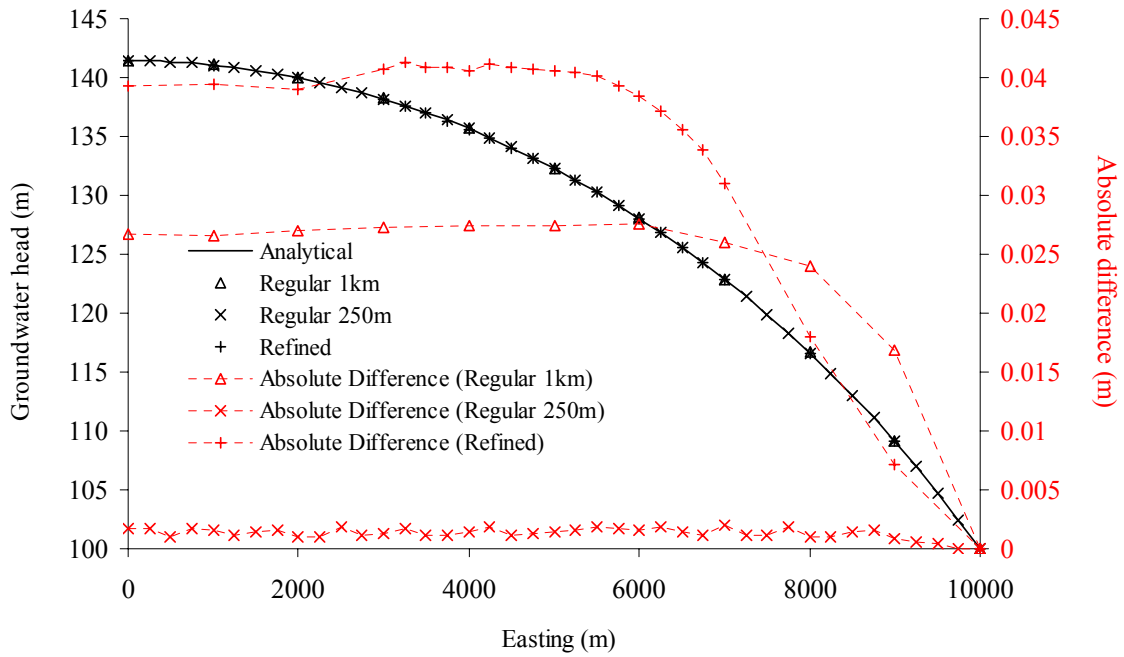


Figure 5 Steady state groundwater head profiles for 1-D model

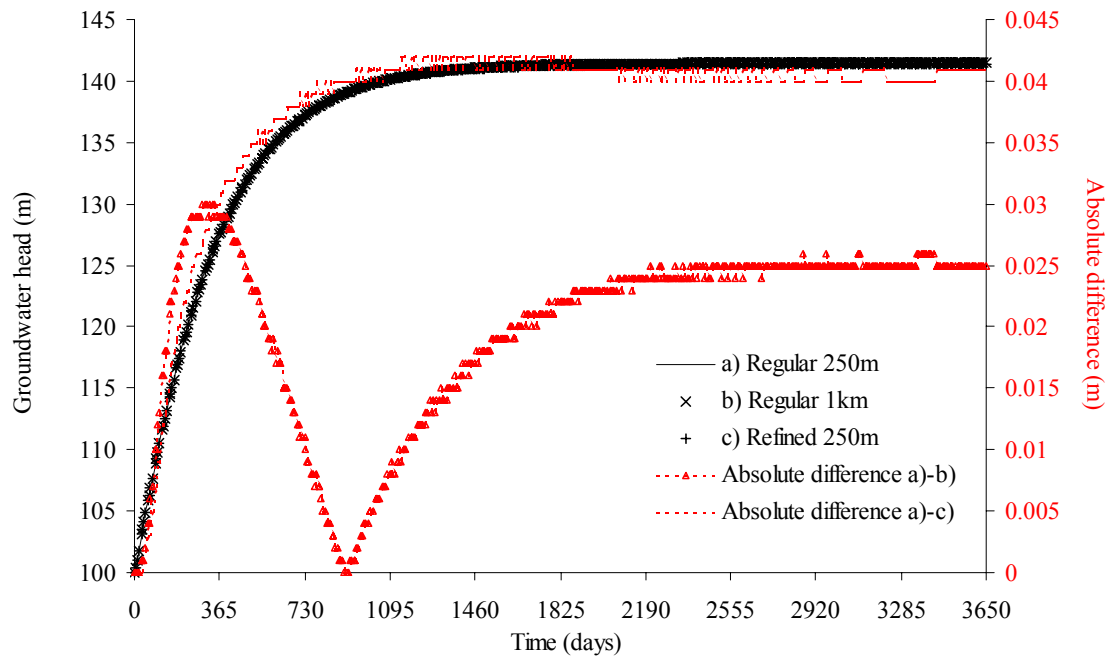


Figure 6 Groundwater hydrographs on western boundary for 1-D models showing progress towards steady state solution

2.2.2 Abstraction in an unconfined aquifer

The accuracy of ZOOMQ3D when simulating unconfined aquifers is also tested using a model centred on a pumped well. The unconfined aquifer is ten kilometres square and has fixed head conditions specified along all boundaries. The boundary head is fixed at 100 m above the base of the aquifer, which is taken as the datum. The solution obtained using a regular fine grid is compared to that computed using a refined grid. The fine grid model contains a uniform regular 250 m square mesh. The refined grid model, shown in Figure 7, is based on a regular base mesh 1 km square. This is refined in the central 4 km square region to a mesh of 250 m square cells. Consequently, the pumped well is simulated at the same scale in both models.

The aquifer is homogeneous and has a hydraulic conductivity of 10 m/day. The specific storage coefficient is set to zero and the specific yield is 0.01. Recharge is applied uniformly over the aquifer at a rate of 1 mm/day. The abstraction well located at the centre of the aquifer pumps water at a constant rate of 20 Ml/day. A two-year period is simulated given an initially flat water table 100 metres above datum.

Comparisons are made between the two models both over time and at the end of the simulation. Figure 8 shows the simulated groundwater head at the pumped well and at the point (3000,5000) over the two-year period. The two models are in close agreement. The maximum absolute difference in groundwater head at the pumped well during the pumping period is 2.4cm. This is equivalent to approximately 0.29% of the drawdown.

Figure 9 shows the groundwater head profiles for the two models at the end of the simulation. The profiles are drawn along the horizontal through the centre of the model, that is, along the line $y = 5000$ m. The maximum absolute head difference at coincident points of the two models along the line is 3.05 cm. This difference occurs at points (2000,5000) and (8000,5000). The two models are in close agreement and the test indicates that the application of the local grid refinement technique to unconfined aquifers is acceptable.

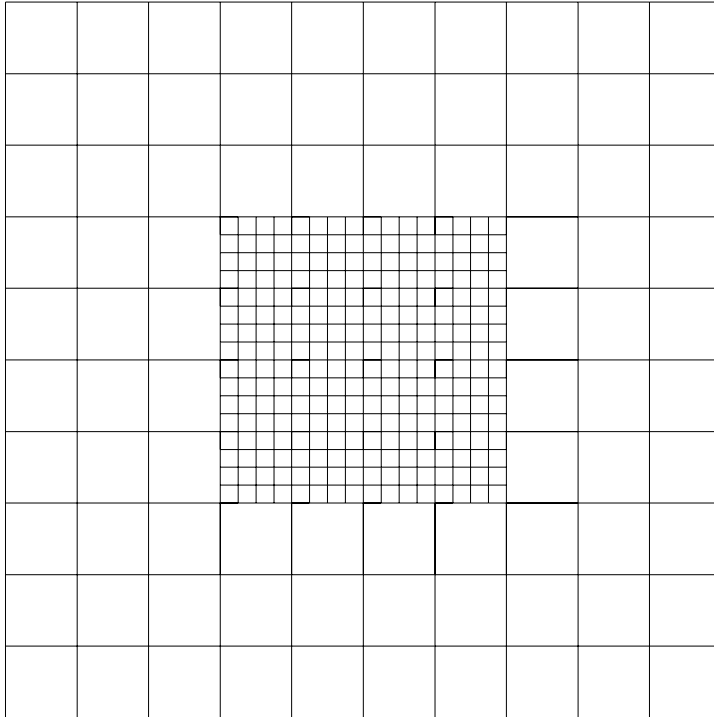


Figure 7 Refined grid model

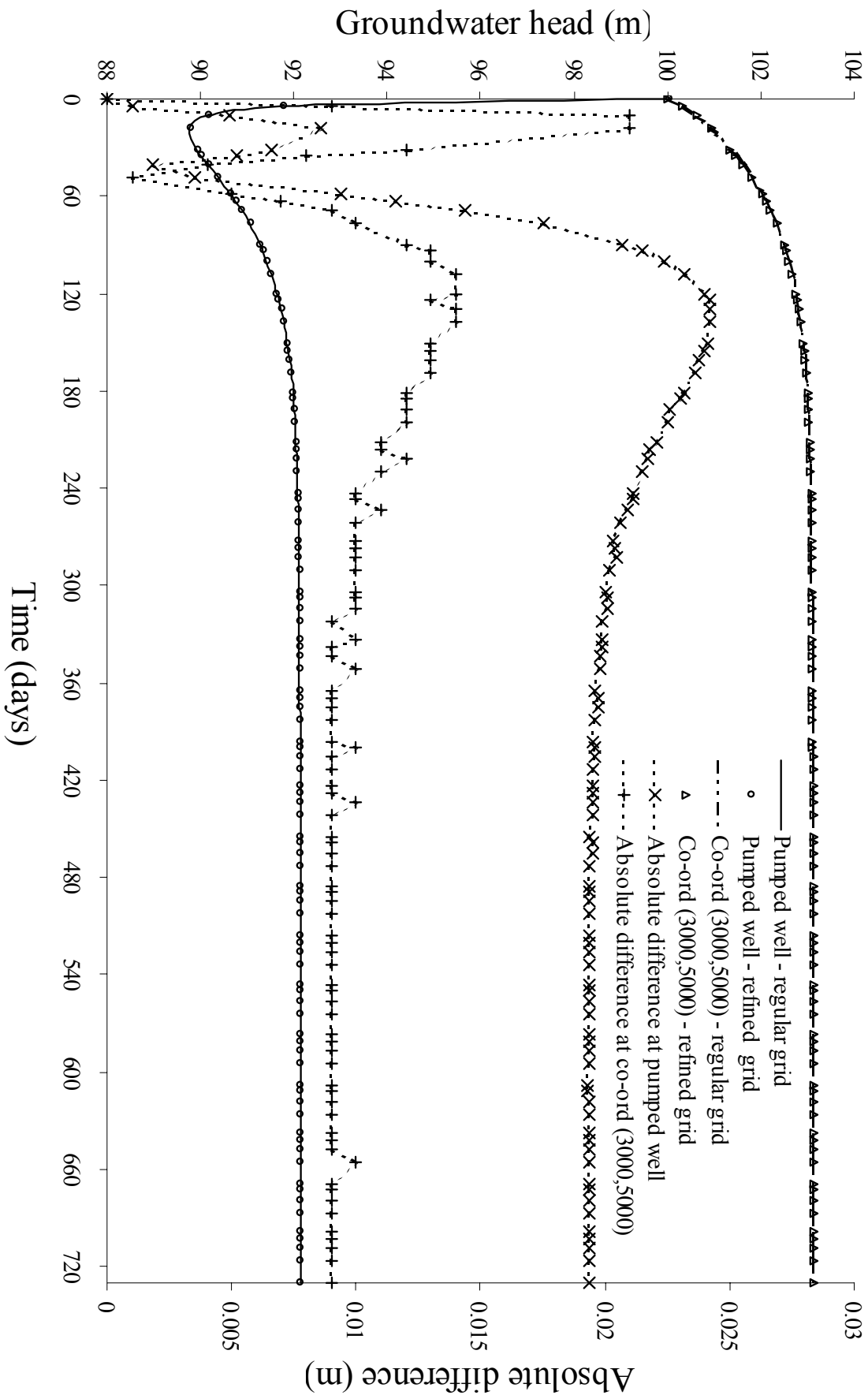


Figure 8 Simulated groundwater head at the pumped well and at the position of the edge of the refined grid by both models

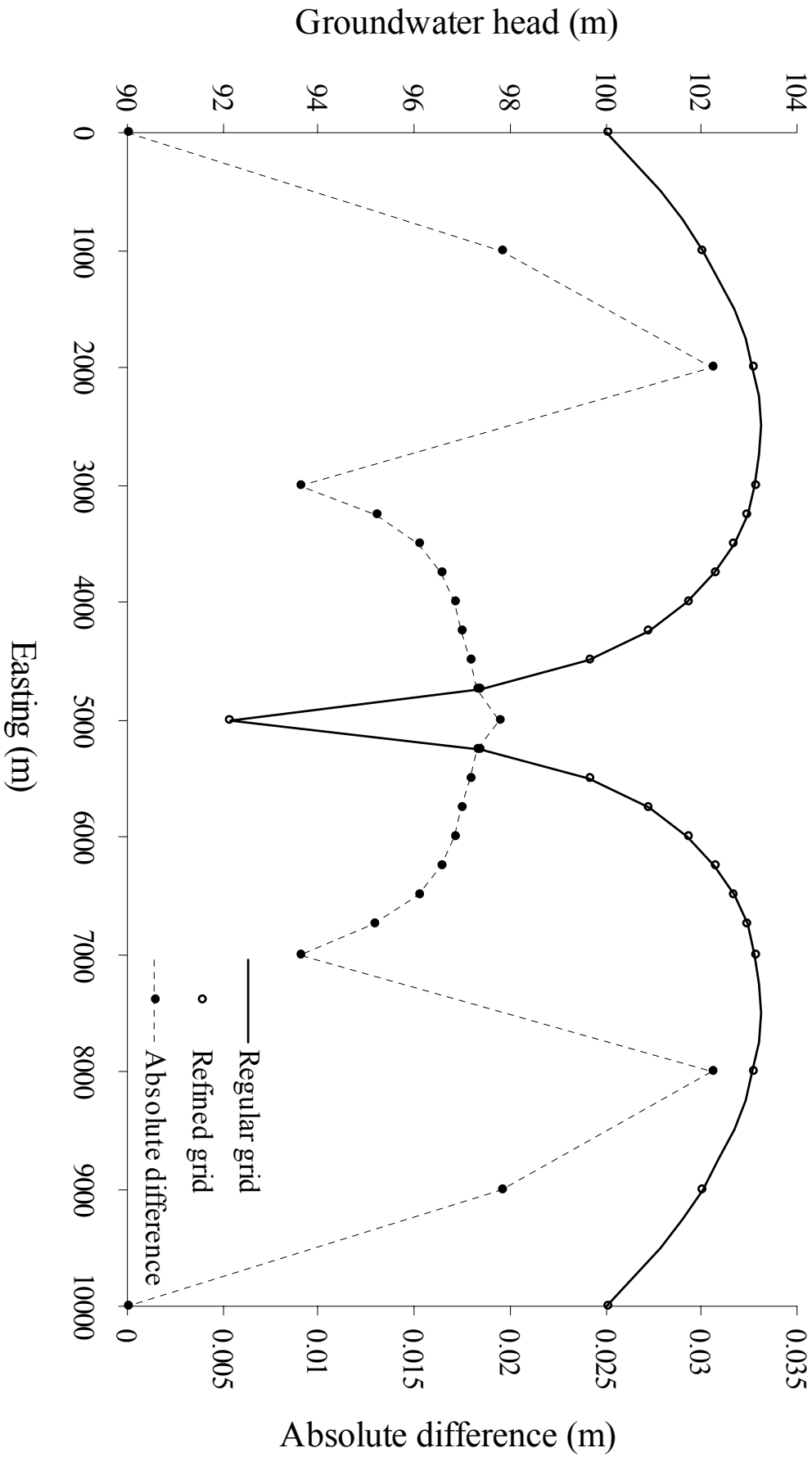


Figure 9 Groundwater head profiles at the end of the two-year simulation period

3 Layers

3.1 REPRESENTATION OF LAYERS IN ZOOMQ3D

Layers are included in the model in the same way that they are incorporated in MODFLOW (McDonald and Harbaugh, 1988). That is, vertical discretisation is implemented by specifying the number of layers and the vertical conductance between them. Because the vertical conductance terms embody the layer thicknesses they are not explicitly included in the finite difference equations. However, the elevations of the layers are required by other model mechanisms. For example, in the Section 5 de-watering and re-wetting of model nodes is discussed. These mechanisms require that the top and bottom elevations of the layers be defined explicitly.

The equations used to calculate the vertical conductance between two nodes are presented in Figure 10, which also shows the two different representations of hydrogeological layers possible within the model. The first illustrates the case where two nodes either fall within a single hydrogeological unit or are located at the midpoints of two vertically adjacent hydrogeological units. The second case illustrates the inclusion of a semi-permeable hydrogeological layer in the model without its explicit representation by a layer of finite difference nodes.

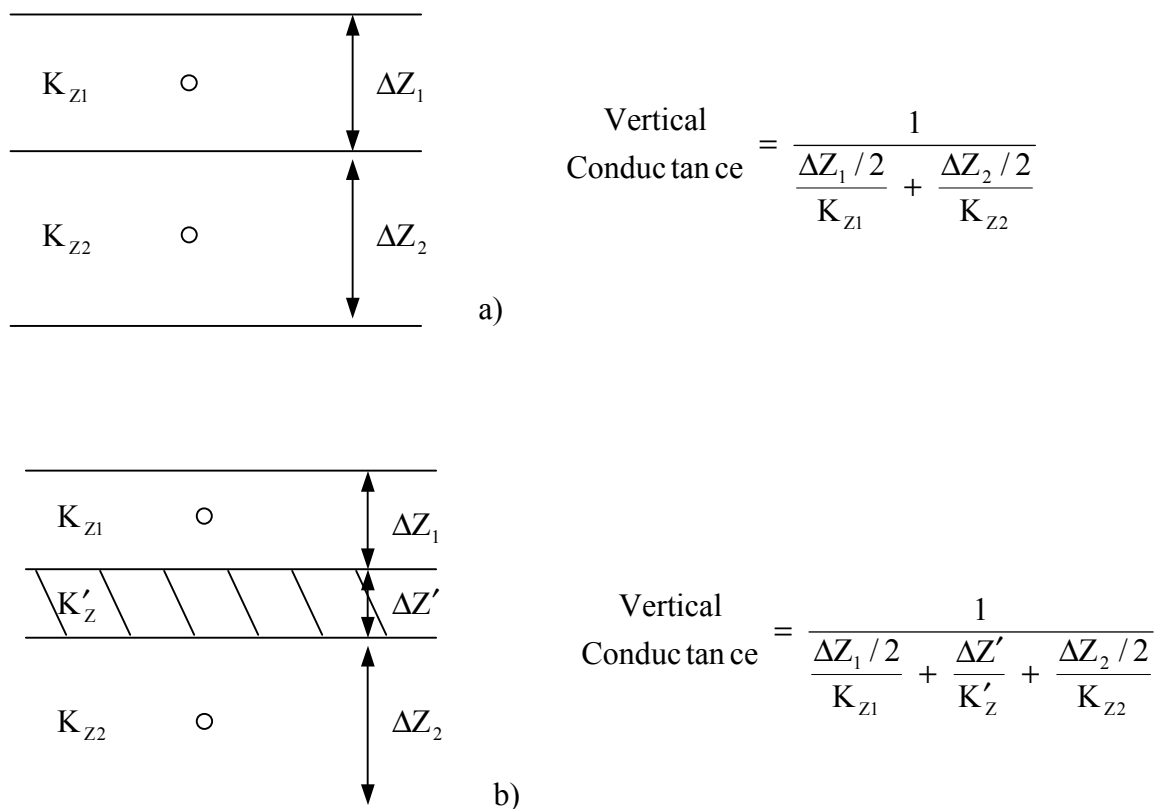


Figure 10 Calculation of the vertical conductance between layers in ZOOMQ3D

A number of tests have been carried out to ensure that the model performs correctly when simulating multiple-layer aquifers. Two tests are described in this section. The first test is based on a problem presented by Anderson (1993), which considers one-dimensional vertical flow. The second uses a model developed by Szekely (1998) as a basis for model validation. Two further tests are described in the later section of this report, in which the representation of

moving boundaries is discussed. There, a mechanism is implemented to handle the de-watering and re-wetting of individual model nodes within single or multiple-layer models.

3.2 ONE DIMENSIONAL VERTICAL FLOW PROBLEM

In this test a vertical one dimensional time-variant flow problem is considered. The test is one of a group of instructional problems designed for MODFLOW by Anderson (1993).

Two 50 m thick aquifers are separated by a 100 m thick semi-permeable hydrogeological layer. Constant head boundary conditions are defined in the upper and lower aquifers of 0 m and -10 m, respectively. Initially the groundwater head in the semi-permeable unit is 0 m. The model is run for one year and the change in head with time is compared between the two models.

The properties of the layers are:

Upper & lower aquifers:	Hydraulic conductivity	1.728 m/day
	Thickness	50 m
	Specific storage	10^{-7} m^{-1}
Semi-permeable layer:	Hydraulic conductivity	$8.64310^{-4} \text{ m/day}$
	Thickness	100 m
	Specific storage	5310^{-6} m^{-1}

Two models are constructed to simulate the system. In the horizontal both are 300 m square with uniform meshes of 100 m square cells. However, the vertical discretisation differs between the two:

Model 1	The aquifers and semi-permeable unit are represented as single layers. A 3 layer, 3 row and 3 column model is therefore set up.
Model 2	The semi-permeable unit is represented by three separate layers of thickness 25 m, 50 m and 25 m. Each aquifer is represented by two layers of 25 m thickness. A 7 layer, 3 row and 3 column model is therefore set up.

The vertical conductances between the model layers are given in Table 1. Layer number increases with depth from the upper layer.

Table 1 Vertical conductances for 1-D vertical flow model

Between layers	Model 1 Vertical Conductance (day^{-1})	Model 2 Vertical Conductance (day^{-1})
1 and 2	1.727568108e-05	0.06912
2 and 3	1.727568108e-05	6.908545e-05
3 and 4	-	2.304e-05
4 and 5	-	2.304e-05
5 and 6	-	6.908545e-05
6 and 7	-	0.06912

Table 2 Drawdowns simulated by MODFLOW and ZOOMQ3D 1-D flow models

Time (Days)	ZOOMQ3D 3 Layer	MODFLOW 3 Layer	ZOOM3D 7 Layer	MODFLOW 7 Layer
0.155	0.053	0.05	0.011	0.01
0.357	0.121	0.12	0.04	0.04
0.62	0.208	0.21	0.098	0.1
0.961	0.319	0.32	0.199	0.2
1.41	0.458	0.46	0.358	0.36
1.98	0.632	0.63	0.591	0.59
2.73	0.847	0.85	0.908	0.91
3.7	1.109	1.11	1.314	1.32
4.97	1.423	1.42	1.798	1.8
6.62	1.789	1.79	2.341	2.34
8.77	2.203	2.2	2.907	2.91
11.6	2.654	2.65	3.455	3.46
15.2	3.124	3.12	3.945	3.95
19.9	3.584	3.58	4.342	4.34
26	4.005	4.01	4.632	4.63
34	4.358	4.36	4.818	4.82
44.3	4.625	4.63	4.922	4.92
57.7	4.806	4.81	4.971	4.97
75.2	4.912	4.91	4.991	4.99
97.9	4.966	4.97	4.998	5
127.5	4.989	4.99	5	5
165.9	4.997	5	5	5
215.8	4.999	5	5	5
280.7	5	5	5	5
365	5	5	5	5

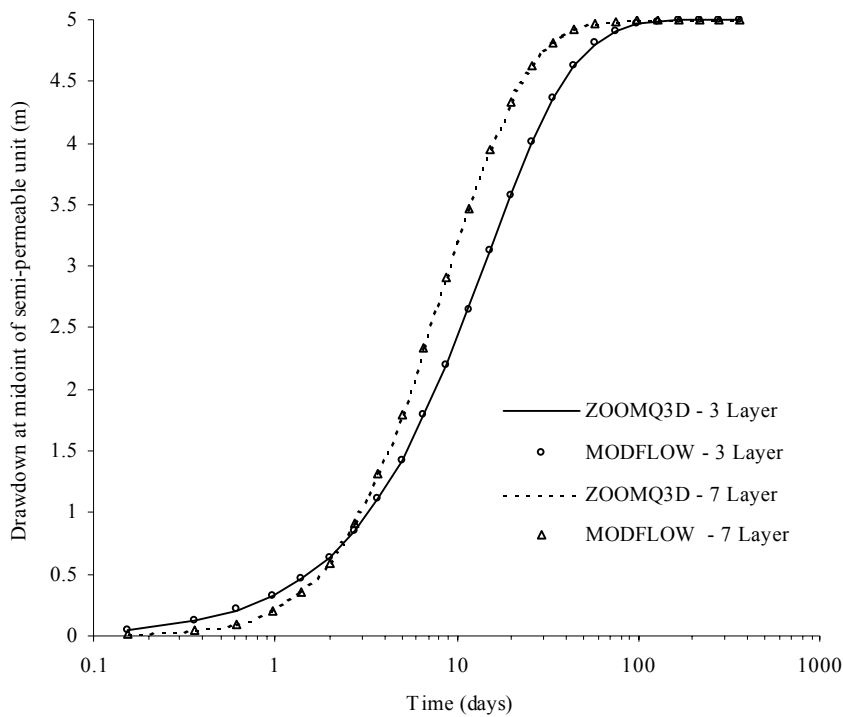


Figure 11 Drawdowns simulated by MODFLOW and ZOOMQ3D 1-D flow models

The groundwater heads simulated at the midpoint of the semi-permeable unit over the one-year period are shown in Table 2 and plotted in Figure 11. The ZOOMQ3D models agree closely with the MODFLOW results presented by Anderson (1993) and show that layering has been introduced correctly within the program code.

3.3 COMPARISON WITH THE MODEL OF SZEKELY (1998)

Szekely (1998) presents a modelling technique, which may be described as a pseudo local grid refinement in that it uses iterative telescopic mesh refinement. The method involves an iterative procedure, which performs repeated scanings across the grid refinement levels to improve the boundary conditions on the grids. The method involves two main numerical procedures: a numerical solution algorithm applied to each grid, or window, and an iterative mesh interface simulator (MIS) to update the boundary conditions. A node-centred finite difference grid is used, as shown in Figure 12, which allows parent and child meshes to be separated along a grid interface containing nodes from both grids.

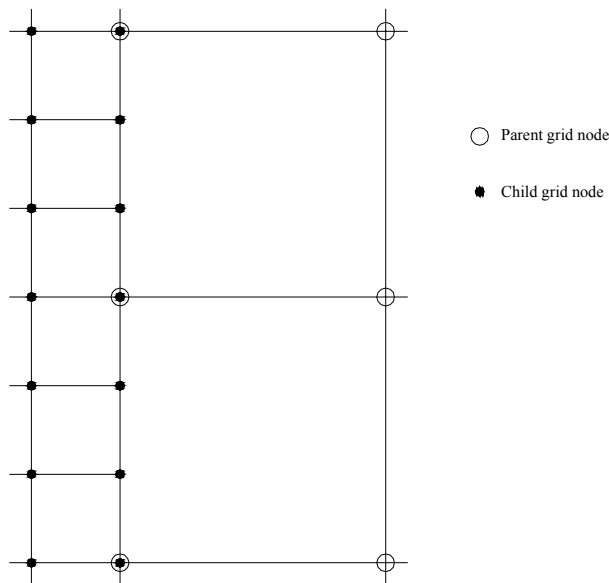


Figure 12 Node-centred grid of Szekely (1998)

A schematic diagram of the steps taken by the numerical algorithm is shown in Figure 13. At each time step of the simulation a series of scans is performed. During each of these scans the solution for groundwater head is computed on all the grids. Starting at the m^{th} scan, a solution is computed on each grid beginning at the finest and progressing to the coarsest mesh. The order in which these solutions is computed is illustrated by the numbers in Figure 13. Each grid is formulated as an initial boundary value problem, that is, they are independent of each other. For the finest grid, fixed head boundary conditions are taken from its parent at the $m-1^{\text{th}}$ scan, linearly interpolating values where necessary. This child grid then provides specified fluxes for internal boundary nodes of its parent. These are calculated by summing the flows to and from the associated fixed head boundary nodes of the child. The subgrid is therefore removed from its parent. The parent's outer fixed head boundary conditions are defined from the grandparent at the previous scanning level and so on. This process continues until a solution has been computed on each grid at the m^{th} scanning level, at which point the $m+1^{\text{th}}$ scan begins. Again, each subgrid's outer fixed head boundary conditions are taken from their parents at the previous scanning level, this time the m^{th} scan. Eventually, the solutions on all the grids converge between scanning levels and the simulation progresses to the next time step. Using this approach the heads along and the fluxes across the interface between two grids are made equal. A result of the repeated scanning procedure is that flux conservation is enforced.

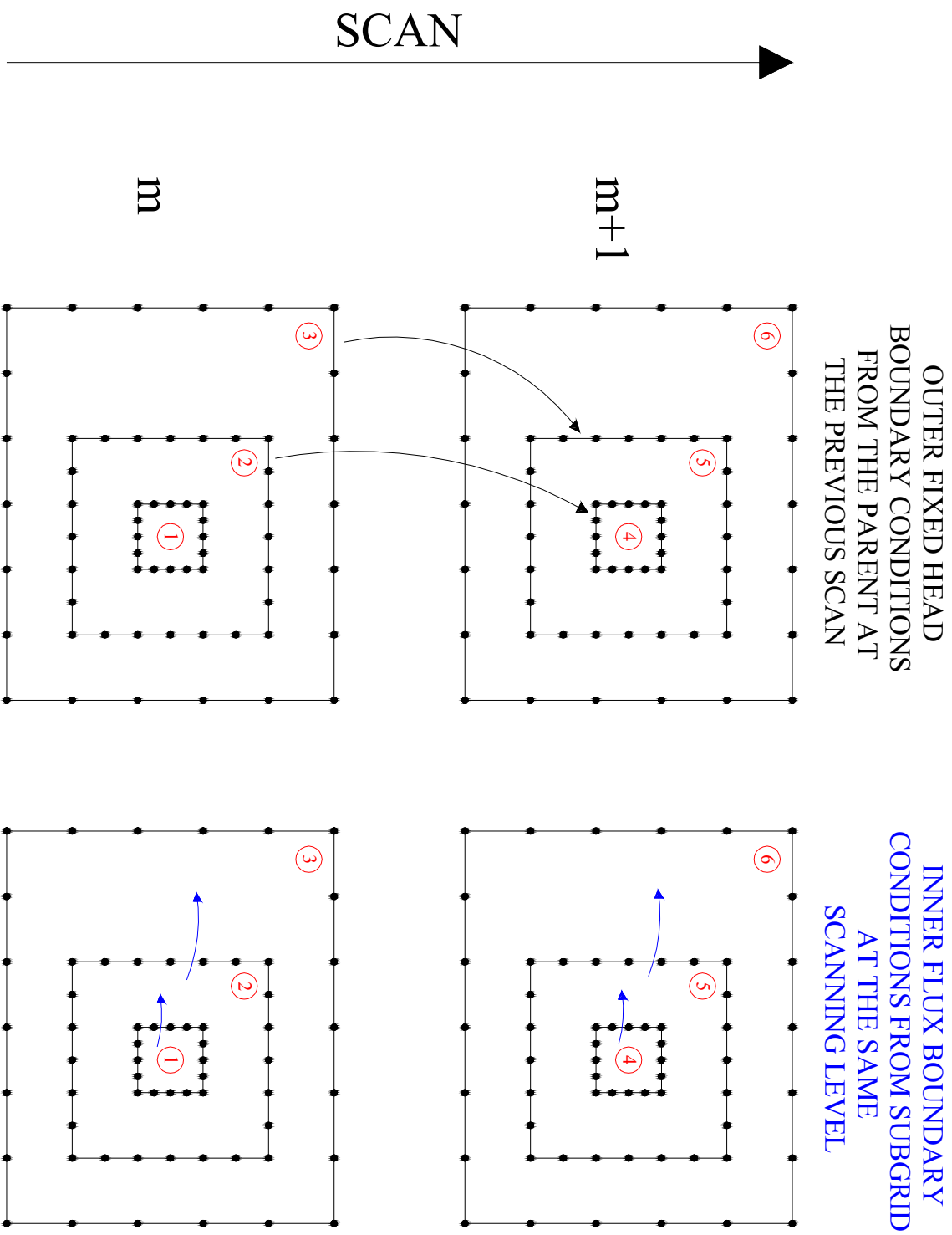


Figure 13 Schematic of the iterative solution procedure of Szekely (1998)

Szekely (1998) validates the model through a comparison with an analytical solution to a steady state doublet well flow problem in a two layer aquifer. An injection and recharge well are placed 80 m apart within the smallest refined grid of the model mesh shown in Figure 14. The aquifer is homogeneous and isotropic. The model parameters are listed in Table 3.

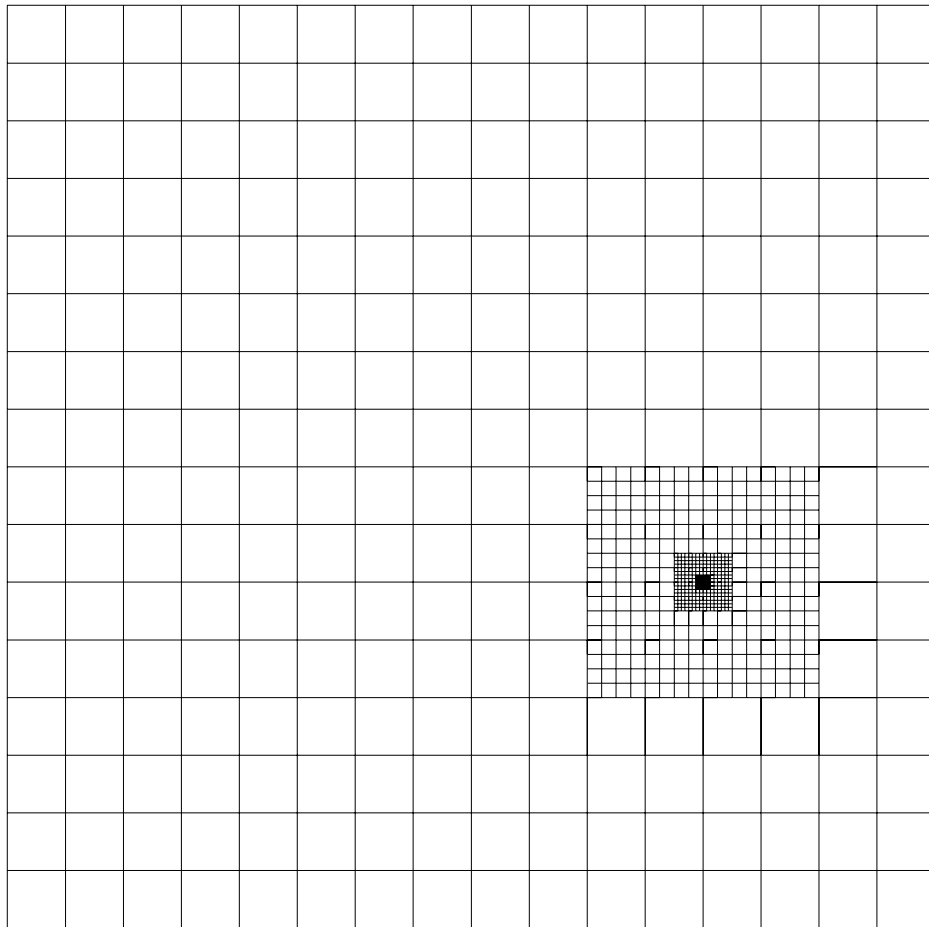


Figure 14 Model mesh of Szekely (1998)

Table 3 Parameters for model presented by Szekely (1998)

	Co-ord SW corner	Co-ord NE corner	Mesh spacing
Base Grid	0,0	10240,10240	640 m x 640 m
1 st refined grid	6400,2560	8960,5120	160 m x 160 m
2 nd refined grid	7360,3520	8000,4160	40 m x 40 m
3 rd refined grid	7600,3760	7760,3920	5 m x 5 m
	Transmissivity	Vertical Conductance	
Layer 1 transmissivity	100 m ² /day	0.001 day ⁻¹	
Layer 2 transmissivity	100 m ² /day		
	Co-ordinate	Pumping rate	
Recharge well	7640,3840	5 MI/day	
Abstraction well	7720,3840	5 MI/day	

An identical model to the one shown in Figure 14 and defined in Table 3 is constructed using ZOOMQ3D. This is used to compute the steady state groundwater head profile. However, it must be noted that the most refined grid violates the ‘rule of thumb’ defined by Jackson (2000) for ZOOMQ3D. This rule states that a model grid should not be refined by more than a factor of five. In Szekely’s test model the mesh spacing is reduced from 40 m to 5 m in the final grid refinement step.

The steady state groundwater head contours simulated by Szekely are plotted in Figure 15. Groundwater heads are compared with the analytical solution at the north west corner of each grid. These are listed in Table 4. The groundwater heads computed by ZOOMQ3D agree closely with the analytical solution and are more accurate than those computed by Szekely’s model. However, it was found that to obtain an accurate solution using ZOOMQ3D the steady state profile had to be computed by simulating the aquifer time-variantly. A 10-year period of abstraction-injection is simulated using a storage coefficient of 10^{-5} .

Setting the storage coefficient to zero introduces small but significant errors into the solution. The magnitude of the errors depends on the selection of the SOR factor, ω . Larger errors are observed with larger values of ω . The variation in the groundwater head profile with different ω may be a result of refining the grid too rapidly, though more investigation is required. It is conceivable that the errors are due to ill-conditioning of the matrix of coefficients of the finite difference equation resulting in round off errors. This could prevent the solution algorithm from calculating the correct and small drawdowns at large distances from the doublet well. The groundwater heads for the ZOOMQ3D simulations are listed in Table 4. The groundwater head contours for the time-variant ZOOMQ3D simulation are plotted in Figure 16.

The computational difficulties associated with the simulation of steady state conditions by setting the storage coefficient to zero should be considered when running a model. The simulation of steady state profiles can occasionally be problematic when this approach is adopted. For greater confidence in the accuracy of the model it is recommended that steady-state conditions are achieved by running the model time-variantly to steady-state using a non-zero storage coefficient.

Table 4 Comparison between analytical solution and Szekely and ZOOMQ3D models

NW Corner of:	Coarse grid	160 m grid	40 m grid	Finest grid
Analytical solution	0.0355	0.086	0.5779	3.4049
Szekely	0.0339	0.0854	0.5783	3.4133
ZOOMQ3D Time variant steady state	0.036	0.087	0.575	3.410
ZOOMQ3D True steady state SOR factor=1.0	0.059	0.11	0.598	3.433

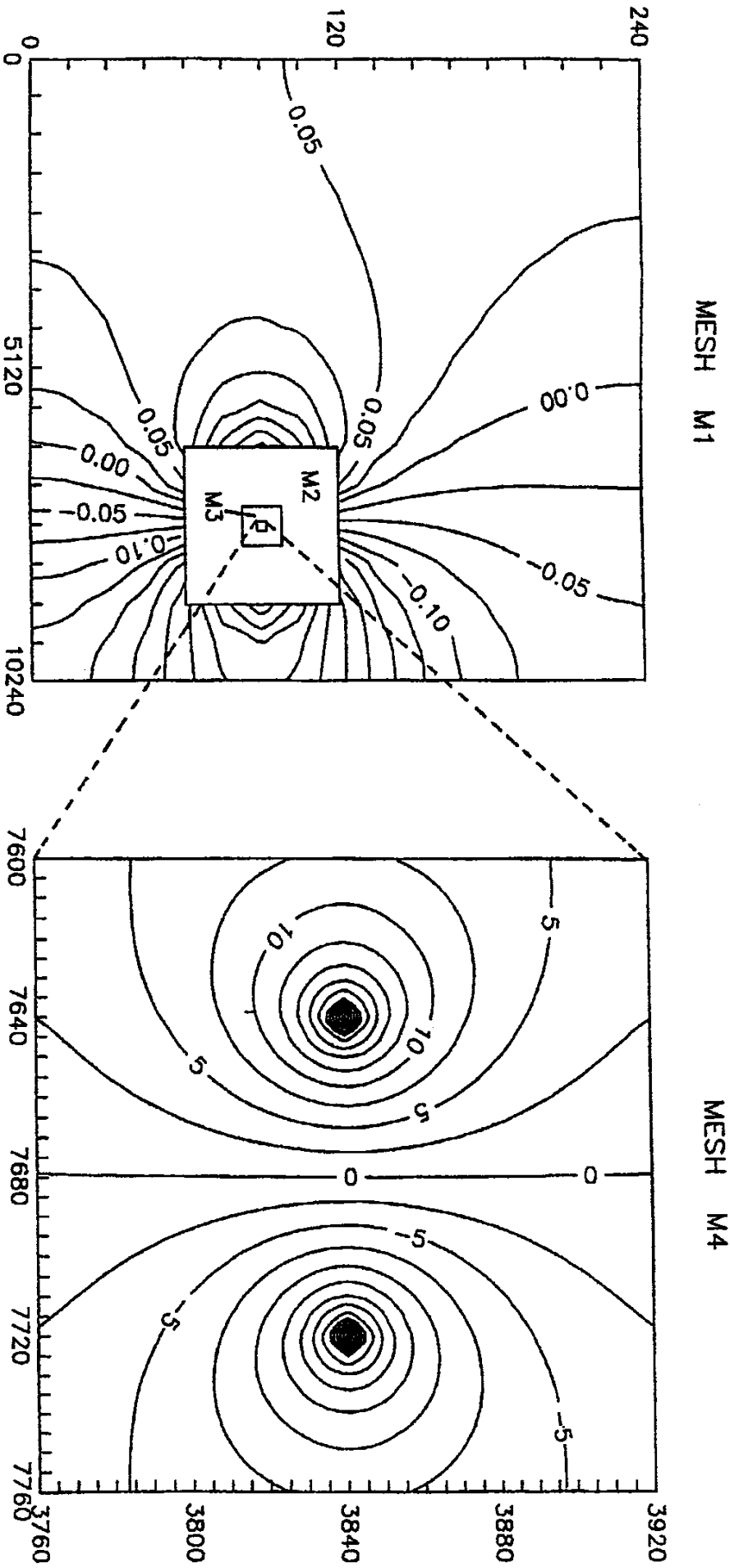


Figure 15 Steady state groundwater head contours after Szekely (1998)

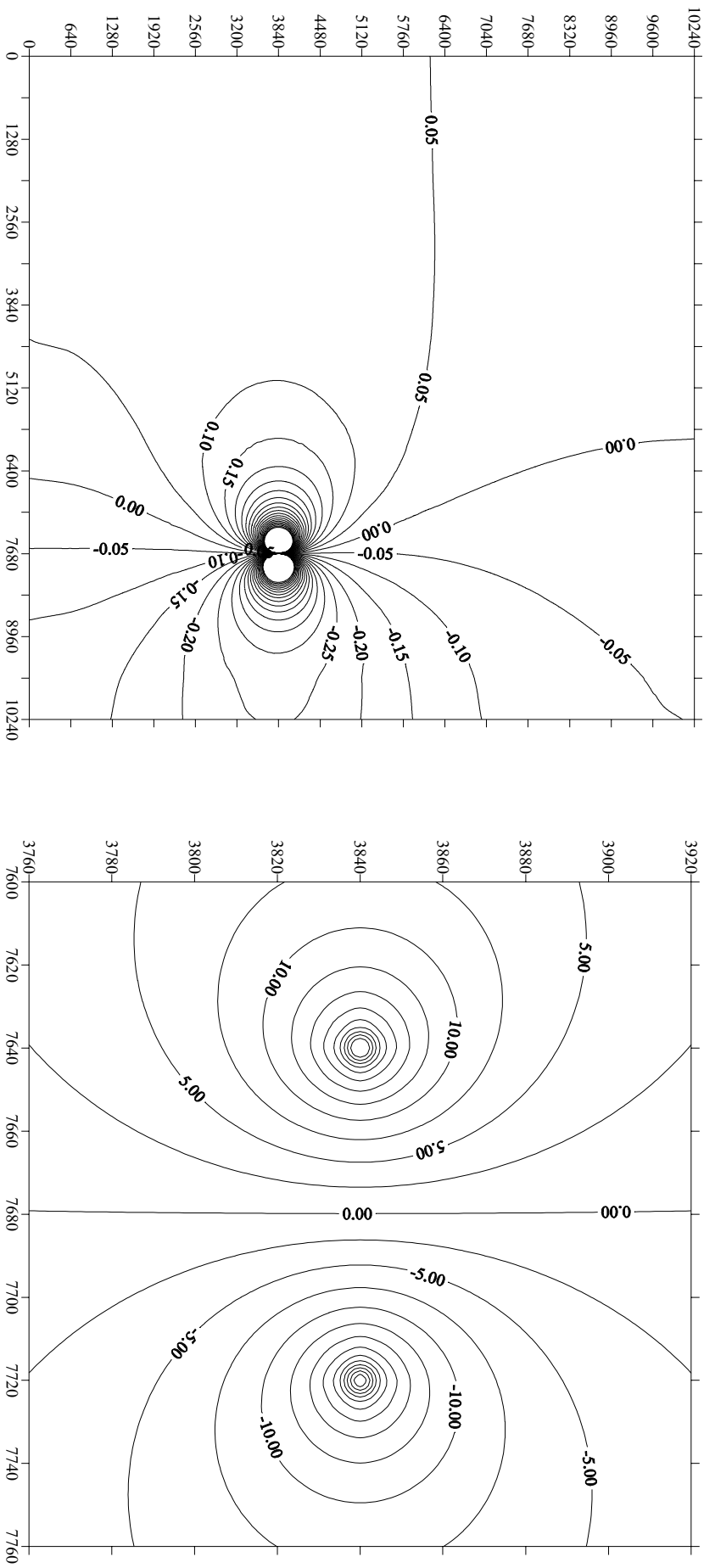


Figure 16 Steady state groundwater head contours computed by ZOOM3D

4 Springs

Springs are usually simulated in models using a head dependent leakage mechanism. This mechanism was already incorporated in the model. However, the conceptualisation of a spring in this way, in which the outflow from the aquifer is based on a ‘bed conductance’ could be argued to be simplistic. Consequently, another spring mechanism has been developed in which spring flows are dependent on the groundwater head in the aquifer, but not governed by a conductance term. Instead, spring flows can only be adjusted by modifying the transmissivity of the aquifer in the region of the spring. Consequently, the general pattern of flow within the aquifer determines the outflow at a spring location.

Spring objects encapsulate a head dependent abstraction mechanism. When simulating unconfined aquifers the transmissivity is updated within a cyclical procedure. The solution for the current time step is computed a number of times within the cyclical process. After each cycle the transmissivity is adjusted (refer to Section 2). Spring flows are also adjusted at the end of each cycle. A spring object is defined by two elevations: the ground level and a level just below the ground surface, for example 0.1 m below the ground surface. If at the end of a cycle the groundwater head is above the ground surface at the spring then the spring is set to a fixed flow. This flow rate is calculated, using the specific yield and time step length, so that the groundwater head is lowered to between the two elevations defined in the spring object. It is given by the equation:

$$Q_s = \left[h - \frac{(Z_G + Z_{SB})}{2} \right] \times \frac{S_y \times \Delta x \times \Delta y}{\Delta t}$$

where:

Q_s is the specified spring flow rate (m³/day),

h is the groundwater head at the spring node (m),

Z_G is the elevation of the ground surface(m),

Z_{SB} is the elevation of the base of the spring (m),

Δx is the width of the node in the x-direction (m),

Δy is the width of the node in the y-direction (m),

S_y is the specific yield and,

Δt is the time step length (days)

Consequently, the spring is set to ‘abstract’ water from the aquifer during the next cycle of the transmissivity/spring flow adjustment procedure. At the end of the next cycle the spring flow is readjusted by examining the groundwater head again. This cyclical procedure terminates and the simulation progresses to the next time step when both the transmissivity and spring flows stop varying between cycles.

The operation of the ‘head dependent flow’ spring objects is validated by examining detailed nodal and global flow balances. These objects are used in the model described in Section 5.4 to represent springs, where they are found to operate in a stable manner.

5 Moving boundaries: node de-watering and re-wetting

5.1 BACKGROUND

In this section the de-watering and re-wetting of nodes within ZOOMQ3D is described. Examples are presented illustrating both the de-watering of layers in multiple-layer models and the movement of a horizontal boundary in a sloping bed aquifer. Two of the tests again show that layers have been incorporated correctly into ZOOMQ3D.

Except for CConfinedNode(s) model nodes can both desaturate and de-water. Desaturation is represented by calculating transmissivity based on the saturated thickness of the node. A node de-waters when the groundwater head falls below the base of the node at which point the node is removed from the matrix of finite difference equations. Recharge is then applied to the node below or the most upper active node if that node has also de-watered. The interaction between rivers and other leakage mechanisms must also be adjusted. This is achieved by adjusting the pointer between the CInteractionNode object and the aquifer. This pointer is made to point to the uppermost active aquifer node. This is a simple operation and is an illustration of one of the benefits of the use of objects and pointers.

Horizontal moving boundaries are dealt with similarly to the vertical de-watering of a layer. Horizontally neighbouring nodes which de-water are removed from the matrix of finite difference equation. No flow is permitted for the next time step. The reintroduction of nodes into the system when they re-wet is discussed in Section 5.4.

5.2 1D STEADY STATE FLOW IN AN UNCONFINED AQUIFER.

The aquifer simulated is 10 km long from west to east. The western boundary is impermeable and the eastern boundary is specified as a constant head boundary with heads fixed at 100 m above the base of the aquifer, which is taken as the datum. The aquifer is unconfined and receives recharge uniformly at a rate of 1 mm/day. It is homogenous and has hydraulic conductivity of 1 m/day.

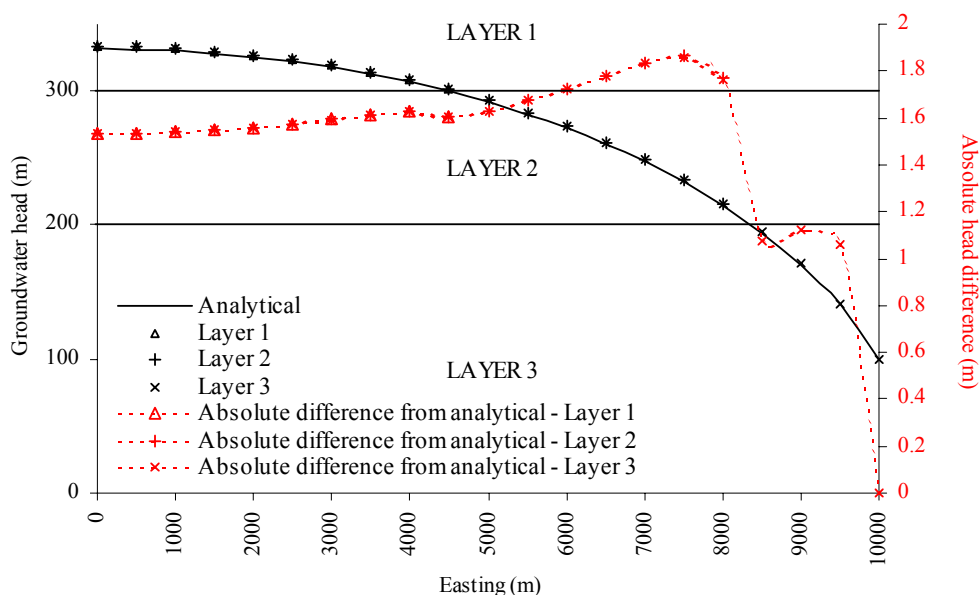


Figure 17 Simulated heads and analytical solution for 1-D flow in unconfined aquifer

The analytical solution to this one-dimensional steady state problem is given in Section 2.2.1. It is the solution to the Dupuit-Forcheimer equation (Rushton, 1979) for this aquifer system with an impermeable left hand boundary and a specified head boundary of the right. The aquifer is simulated using 21 columns, 2 rows and 3 layers of finite difference nodes. In the horizontal x-direction the 10 km aquifer is divided into twenty 500 m mesh intervals. In the y-direction the aquifer is divided into one 500 m mesh interval. The three model layers are horizontal and their base elevations are 0 m, 200 m and 300 m above the datum. The vertical conductance is the same between all the layers and is set at 1.0 day^{-1} . A relatively large value is used to minimise vertical components of flow, which the analytical solution to the Dupuit-Forcheimer equation ignores.

The simulated steady state groundwater heads are plotted against the analytical solution in Figure 17. These agree satisfactorily. The top layer, layer 1, de-waters from easting 5000 m. Layer 2 de-waters from easting 8500 m. The accuracy of the computed solutions indicates that the de-watering mechanism has been incorporated correctly in ZOOMQ3D. However, there are greater differences in head between the model and analytical solution in layer 2. These differences can be reduced by increasing the number of finite difference mesh intervals in the model.

5.3 VERTICAL SLICE THROUGH A MULTI-LAYERED AQUIFER

Anderson (1993) presents an instructional test problem for MODFLOW (McDonald and Harbaugh, 1988) based on a multi-layer aquifer. This model is used to test for the correct operation of ZOOMQ3D's de-watering mechanism. The MODFLOW model is illustrated in Figure 18. It consists of a multi-layer vertical slice near a river represented by a constant head boundary in the upper right hand corner of the domain. The model contains six layers and 27 columns. The layer thicknesses are variable and layers D and E pinch out towards the eastern boundary. Horizontal grid spacing is uniform at 1050 m.

The left hand boundary is specified by a groundwater divide. On the right, the river is assumed to penetrate layers 1, 2 and 3 and is represented by constant heads of 290 m. The remainder of the right hand boundary apart from layer 6 is impermeable. The heads in layer 6 are fixed to allow leakage into and out of the overlying system. The constant heads in layer 6 are listed in Table 5. The upper boundary is the water table, which receives recharge at a rate of 0.30023 mm/day. Recharge is applied to the highest active node. The groundwater head at the variable head nodes is initially 500 m above the datum.

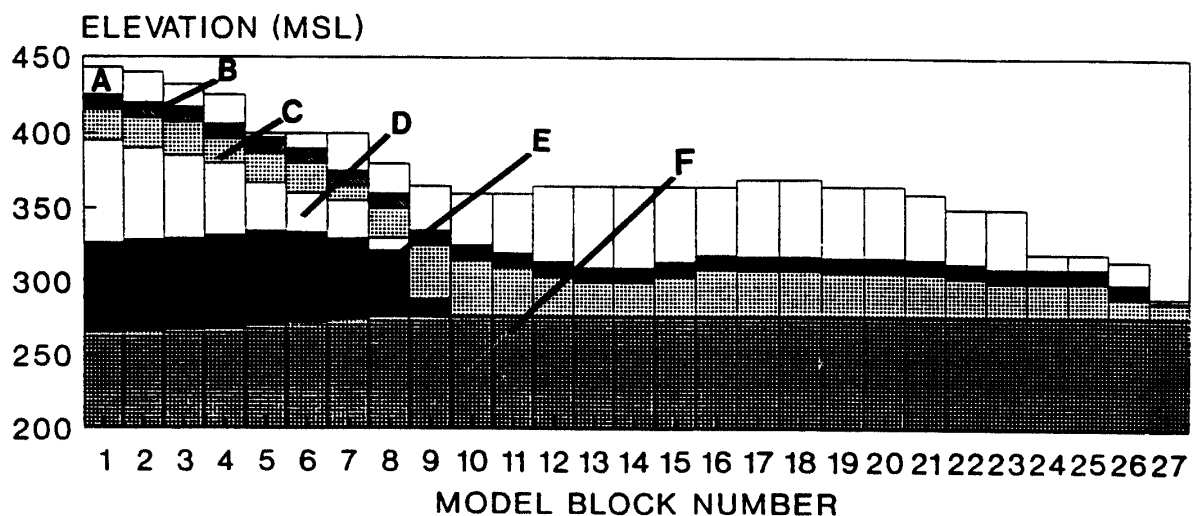


Figure 18 Multi-layer MODFLOW model presented by Anderson (1993)

The base elevation, horizontal hydraulic conductivity and vertical conductance for each block are specified in Table 6. When calculating the vertical conductance a horizontal to vertical hydraulic conductivity anisotropy ratio of 10 to 1 is assumed.

A ZOOMQ3D model is constructed, which is similar but not identical to the MODFLOW model shown in Figure 18. The difference is because ZOOMQ3D is node-centred whilst MODFLOW is block-centred. The ZOOMQ3D model contains 27 columns, 3 rows and 6 layers of finite difference nodes. Therefore, there are 26 and 2 mesh intervals in the x and y-directions respectively. The horizontal mesh is composed of uniform square cells of size 1050 m. In the x-direction, the finite difference nodes of ZOOMQ3D coincide with the left hand cell walls of the MODFLOW blocks. Consequently, the right hand boundary is represented slightly differently in each model. However, the elevations and hydraulic parameters of ZOOMQ3D's nodes are identical to those of the corresponding MODFLOW block.

This example model is used to test the implementation of moving boundaries within ZOOMQ3D because the nodes in the upper left hand corner of the model are dry in the steady state solution. Certain nodes de-water in both layer 1 and layer 2.

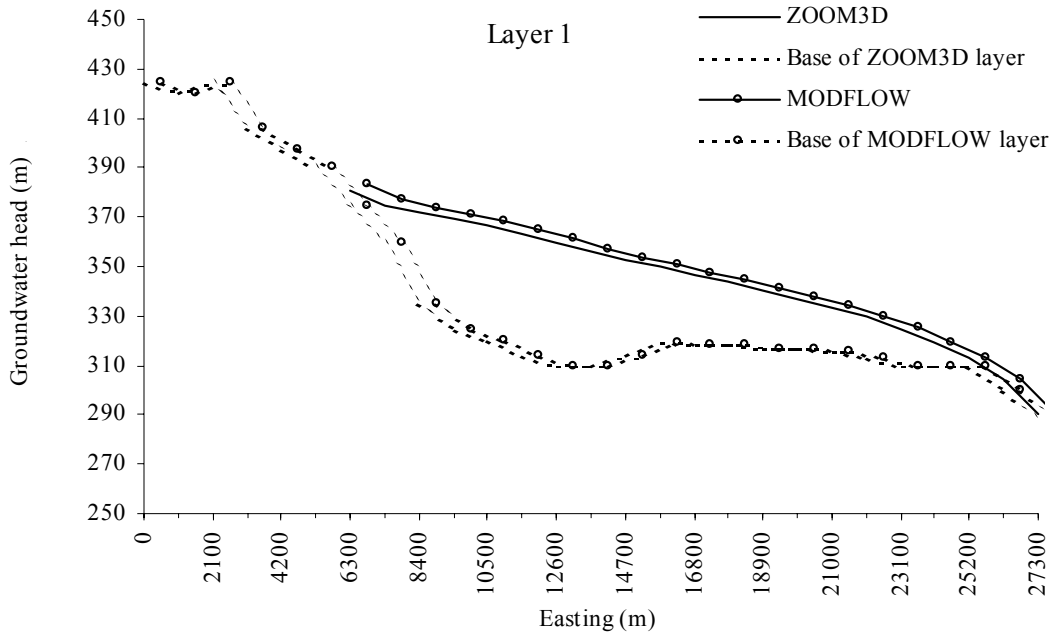
The steady state solution is computed by both setting the storage coefficient to zero and by simulating a number of years of constant recharge using a realistic storage coefficient value. Initial conditions are varied but found to have no effect on the final solution. A fully saturated aquifer and an aquifer with de-watered upper layers are both used as initial conditions. All ZOOMQ3D simulations compute the same steady state profile, which is in close agreement with the MODFLOW model. The simulated groundwater head profiles are shown in Figure 19 for each layer. The differences between the two models are due to the fact that ZOOMQ3D is *grid-centred* and MODFLOW is *block-centred*. Consequently, positions of the ZOOMQ3D nodes and MODFLOW blocks are slightly different. In Figure 19f the groundwater head profile computed by ZOOMQ3D in layer 1 is shifted by half a mesh interval, which shows the similarity of the profile more clearly.

Table 5 Specified heads in layer six of multi-layer MODFLOW model

Column Number	Fixed head (m)
1	320
2	319.6
3	319.2
4	318.8
5	318.5
6	318.1
7	317.7
8	317.3
9	316.9
10	316.5
11	316.2
12	315.8
13	315.4
14	315
15	314.6
16	314.2
17	313.9
18	313.5
19	313.1
20	312.7
21	312.3
22	311.9
23	311.5
24	311.2
25	310.8
26	310.4
27	310

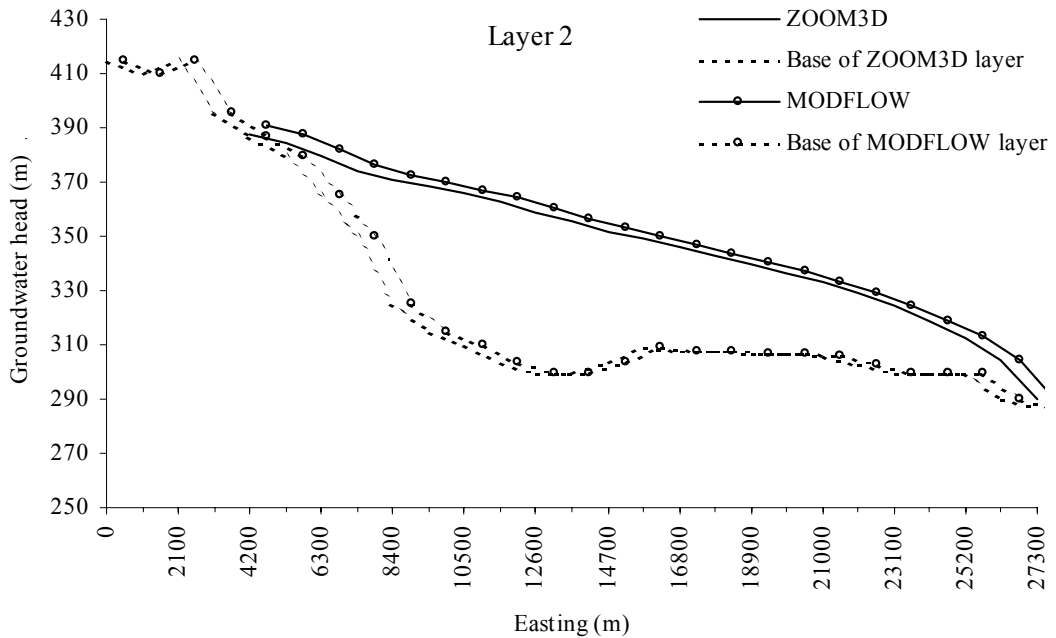
Table 6 Parameter values for the six-layer MODFLOW model

Col	Top Elevation						Base Elevation of Layer						Horizontal Hydraulic Conductivity of Layer						Vertical Conductance					
	Layer 1	1	2	3	4	5	6	1	2	3	4	5	6	1	2	3	4	5	6	Layer 1-2	Layer 2-3	Layer 3-4	Layer 4-5	Layer 5-6
1	450	425	415	395	327	265	200	0.28	0.028	28	0.28	0.000028	0.0028	0.00048	0.00058882	0.00082114	9.03127E-08	8.93855E-08						
2	440	420	410	390	329	266	200	0.28	0.028	28	0.28	0.000028	0.0028	0.000466667	0.000558882	0.000915033	8.88803E-08	8.79677E-08						
3	440	425	415	385	330	267	200	0.28	0.028	28	0.28	0.000028	0.0028	0.000486957	0.000558325	0.001012658	8.88811E-08	8.79535E-08						
4	425	406	396	380	332	268	200	0.28	0.028	28	0.28	0.000028	0.0028	0.000470588	0.000559105	0.001162791	8.74934E-08	8.65801E-08						
5	400	397	387	367	335	270	200	0.28	0.028	28	0.28	0.000028	0.0028	0.000543689	0.000558882	0.00173913	8.61496E-08	8.52359E-08						
6	400	390	380	360	334	272	200	0.28	0.028	28	0.28	0.000028	0.0028	0.000509091	0.000558882	0.002137405	9.03188E-08	8.92857E-08						
7	400	375	365	355	330	274	200	0.28	0.028	28	0.28	0.000028	0.0028	0.000448	0.000559441	0.002231076	9.99955E-08	9.86958E-08						
8	380	360	350	330	322	276	200	0.28	0.028	28	0.28	0.000028	0.0028	0.000466667	0.000558882	0.006829268	1.21737E-07	1.1976E-07						
9	365	335	325	290	289	276	200	0.28	0.028	28	0.28	0.000028	0.0028	0.000430769	0.000558047	0.041481481	4.30766E-07	4.06977E-07						
10	360	325	315	277	277	276	200	0.28	0.028	28	28	0.0028	0.0028	0.000414815	0.00055788	0.145454545	5.6	7.36842E-06						
11	360	320	310	277	277	276	200	0.28	0.028	28	28	0.0028	0.0028	0.0004	0.000558158	0.167164179	5.6	7.36842E-06						
12	365	314	304	277	277	276	200	0.28	0.028	28	28	0.0028	0.0028	0.000370861	0.000558492	0.203636364	5.6	7.36842E-06						
13	365	310	300	277	277	276	200	0.28	0.028	28	28	0.0028	0.0028	0.00036129	0.000558715	0.238297872	5.6	7.36842E-06						
14	365	310	300	277	277	276	200	0.28	0.028	28	28	0.0028	0.0028	0.00036129	0.000558715	0.238297872	5.6	7.36842E-06						
15	365	314	304	277	277	276	200	0.28	0.028	28	28	0.0028	0.0028	0.000370861	0.000558492	0.203636364	5.6	7.36842E-06						
16	365	319	309	277	277	276	200	0.28	0.028	28	28	0.0028	0.0028	0.000383562	0.000558214	0.172307692	5.6	7.36842E-06						
17	370	318	308	277	277	276	200	0.28	0.028	28	28	0.0028	0.0028	0.000368421	0.000558269	0.177777778	5.6	7.36842E-06						
18	370	318	308	277	277	276	200	0.28	0.028	28	28	0.0028	0.0028	0.000368421	0.000558269	0.177777778	5.6	7.36842E-06						
19	365	317	307	277	277	276	200	0.28	0.028	28	28	0.0028	0.0028	0.000378378	0.000558325	0.183606557	5.6	7.36842E-06						
20	365	317	307	277	277	276	200	0.28	0.028	28	28	0.0028	0.0028	0.000378378	0.000558325	0.183606557	5.6	7.36842E-06						
21	360	316	306	277	277	276	200	0.28	0.028	28	28	0.0028	0.0028	0.000388889	0.000558381	0.189830508	5.6	7.36842E-06						
22	350	313	303	277	277	276	200	0.28	0.028	28	28	0.0028	0.0028	0.000408759	0.000558548	0.211320755	5.6	7.36842E-06						
23	350	310	300	277	277	276	200	0.28	0.028	28	28	0.0028	0.0028	0.0004	0.000558715	0.238297872	5.6	7.36842E-06						
24	320	310	300	277	277	276	200	0.28	0.028	28	28	0.0028	0.0028	0.000509091	0.000558715	0.238297872	5.6	7.36842E-06						
25	320	310	300	277	277	276	200	0.28	0.028	28	28	0.0028	0.0028	0.000509091	0.000558715	0.238297872	5.6	7.36842E-06						
26	315	300	290	277	277	276	200	0.28	0.028	28	28	0.0028	0.0028	0.000486957	0.000559273	0.414814815	5.6	7.36842E-06						
27	290	288	287	277	277	276	200	0.28	0.028	28	28	0.0028	0.0028	0.004666667	0.005544554	0.533333333	5.6	7.36842E-06						



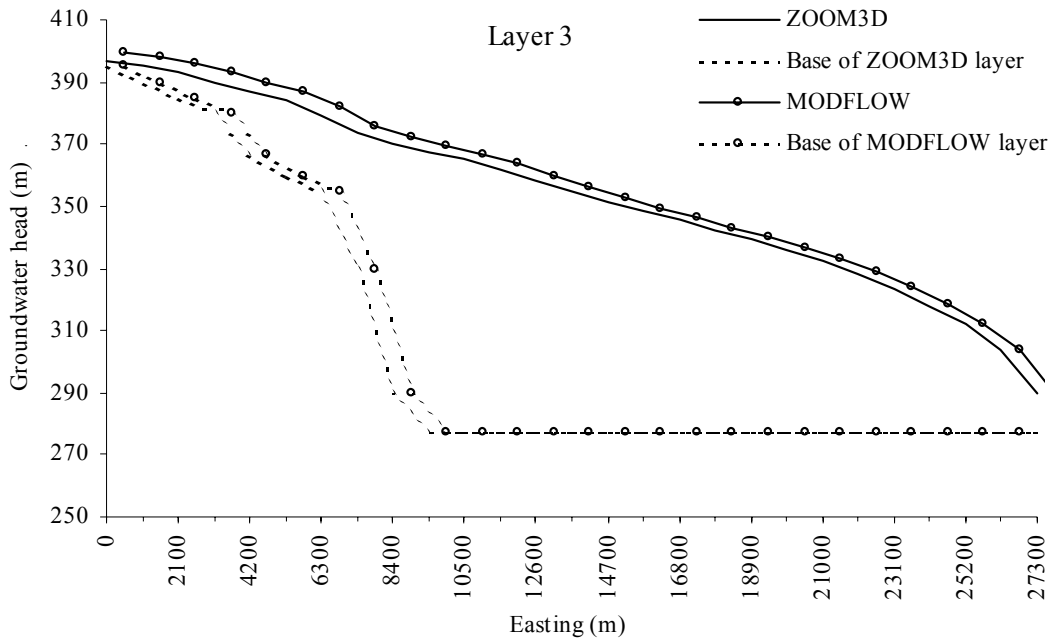
a)

Figure 19 Comparison between MODFLOW and ZOOMQ3D simulated heads Layer 1 showing de-watering adjacent to western boundary



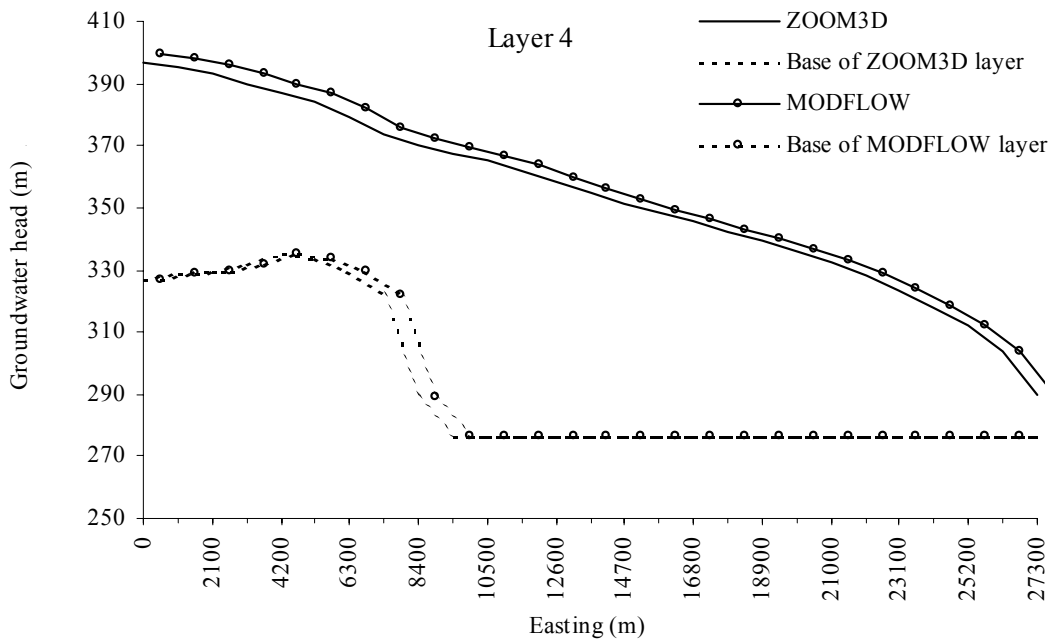
b)

Figure 19b) Comparison between MODFLOW and ZOOMQ3D simulated groundwater heads in layer 2



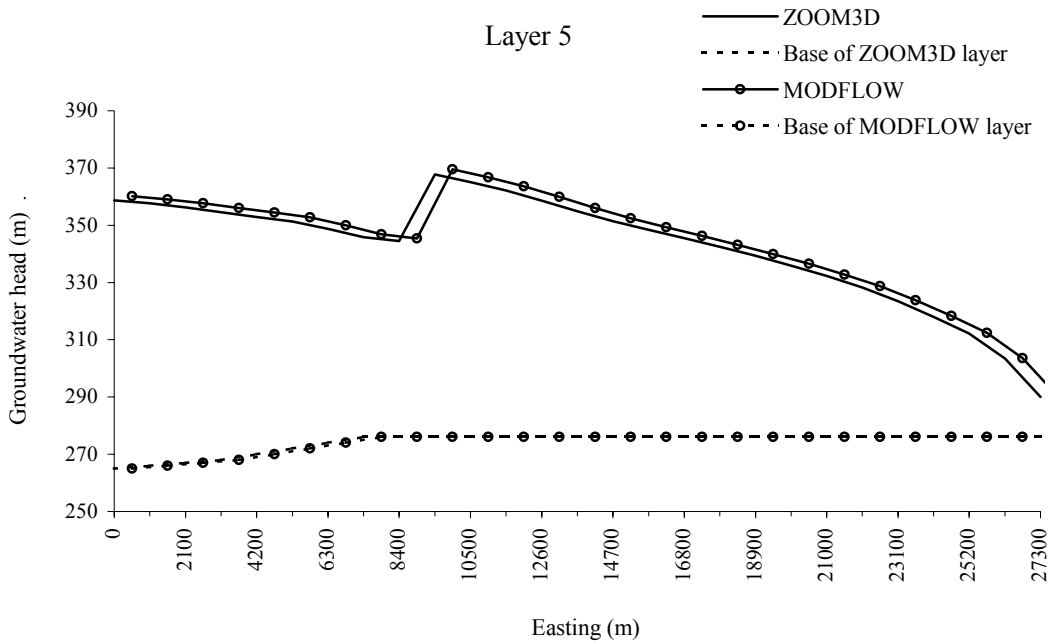
c)

Figure 19c) Comparison between MODFLOW and ZOOMQ3D simulated groundwater heads in layer 3



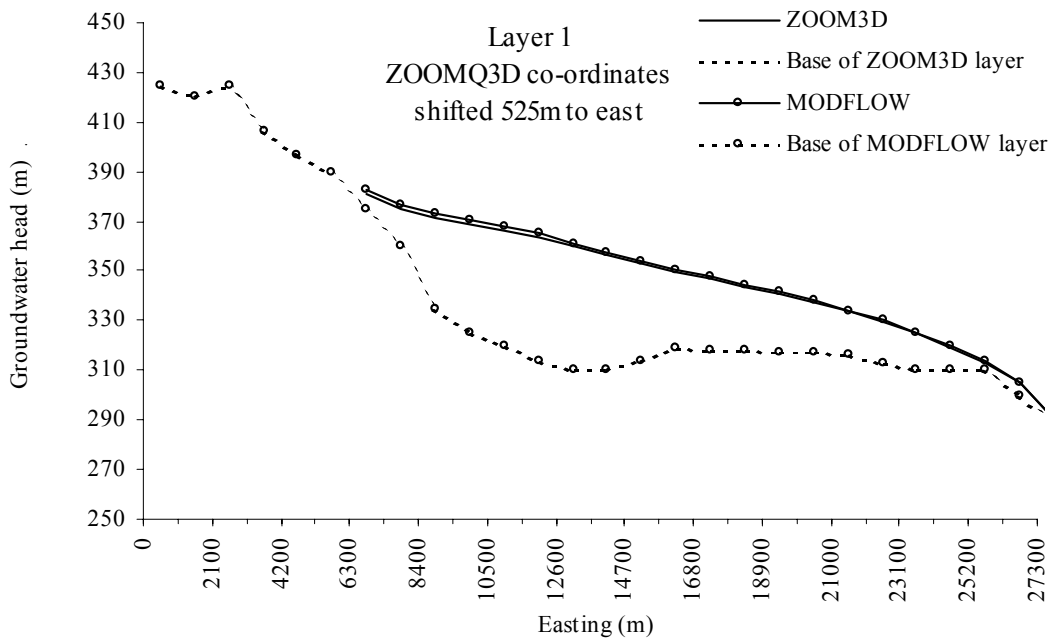
d)

Figure 19d) Comparison between MODFLOW and ZOOMQ3D simulated groundwater heads in layer 4



e)

Figure 19e) Comparison between MODFLOW and ZOOMQ3D simulated groundwater heads in layer 5



f)

Figure 19f) Comparison between MODFLOW and ZOOMQ3D simulated groundwater heads in layer 1. ZOOMQ3D shifted eastwards by 1050 m to aligned node and block centres

5.4 MOVING BOUNDARY IN A SLOPING BED AQUIFER

Model nodes de-water when the groundwater head falls below their base elevation. When this occurs the node is made *inactive* and is removed from the matrix of finite difference equations. A mechanism is implemented to re-wet nodes when groundwater levels rise again. The mechanism is based on the examination of the groundwater head at the neighbouring nodes of the inactive node. Two options are defined. Either the horizontally adjacent nodes can be examined or the node on the layer beneath can be interrogated to determine if the de-watered node should be reactivated.

Three additional parameters are defined in CConvertibleNode objects to allow the re-wetting of nodes (note that CConfinedNode objects cannot de-water and re-wet). These parameters are:

- a wetting flag
- a wetting threshold
- a post wetting head value

The wetting flag is a character variable which is either an 'h' or a 'v'. If it is an 'h' (horizontal) then the inactive node's neighbours on the same layer are examined to determine if their head has risen above the wetting threshold. If it is a 'v' (vertical) then the inactive node's neighbour on the layer below is examined to determine if its head has risen above the wetting threshold. If any of the interrogated neighbouring node's heads are above the wetting threshold then the dry node is reactivated or re-wetted. On re-wetting the groundwater head of the previously inactive node is set to the value stored by the post wetting head variable. The wetting threshold and post wetting head variables are defined as elevations above the base of the node. This method of simulating moving boundaries is identical to that adopted in MODFLOW. A detailed description of the application of the method is given by McDonald et al. (1991).

To test the horizontal de-watering and re-wetting of model nodes a one layer sloping bed model is constructed. This is shown in Figure 20. The aquifer is 10 km long and dips to the east with a slope of 1/100. All model boundaries are impermeable except the upper boundary between eastings 0 m and 8000 m which is defined by the water table. The aquifer is confined to the east of easting 8000 m. Recharge is applied to the unconfined section of the aquifer using a sinusoidal cycle with a frequency of one year. The monthly recharge rates are shown in Table 7 and the recharge pattern is the same for each year of the simulation. The aquifer is homogeneous and isotropic with hydraulic conductivity, specific storage and specific yield of 5.0 m/day, 10^{-5} m^{-1} and 0.05, respectively.

The operation of the de-watering/re-wetting mechanism is tested by examining detailed flow balances at the end of each time step of the simulation. The simulation is also designed to test that the model approaches dynamic balance conditions. The progression of the simulation to a dynamic balance is shown in Figures 21 and 22. Figure 21 shows groundwater head hydrographs at 2 km intervals across the aquifer. At easting 0 m, the aquifer is dry for approximately two thirds of the year. The aquifer also de-waters at easting 2000 m, though for a shorter period of time. The maximum and minimum groundwater head profiles are shown in Figure 20 and are reasonable. The stable nature of progression of the groundwater hydrographs to a dynamic balance indicates that the model is operating correctly. However, it is only through the detailed examination of the nodal and the global flow balances that the model is rigorously validated. Nodal flow imbalances are observed to be of the same magnitude as the convergence criterion, which is assigned a small value.

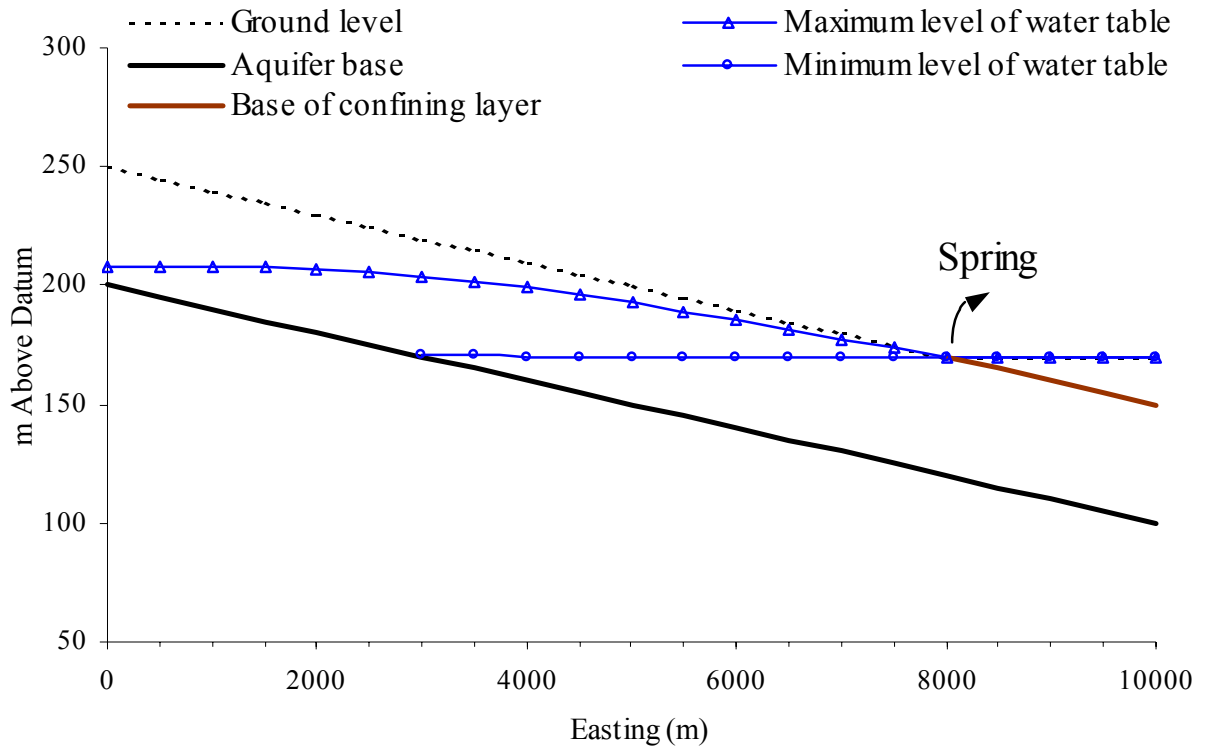


Figure 20 1-D Sloping bed model of unconfined/confined aquifer

Table 7 Monthly recharge rates (mm/day) for sloping bed model

Jan	Feb	Mar	Apr	May	June
0.37	0.40	0.37	0.30	0.20	0.10
July	Aug	Sep	Oct	Nov	Dec
0.03	0.0	0.03	0.10	0.20	0.30

Figure 22 shows the flow rate of the spring located at the unconfined/confined boundary at easting 8000 m. The graph also indicates that the model has reached a dynamic balance and it is consistent with the groundwater hydrographs. Figures 21 and 22 appear to show that the model starts from close to dynamic balance conditions. This is because the initial conditions are a steady state profile simulated using a recharge rate of 0.2 mm/day, which is the average of the monthly values listed in Table 7.

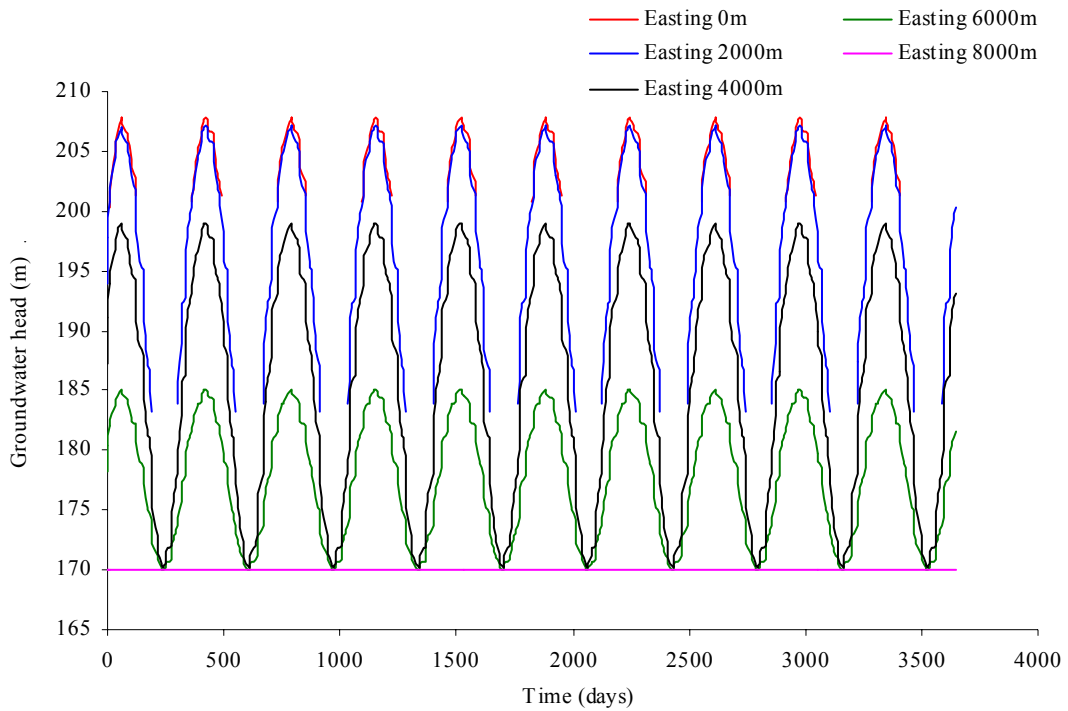


Figure 21 Groundwater hydrographs for unconfined sloping bed model

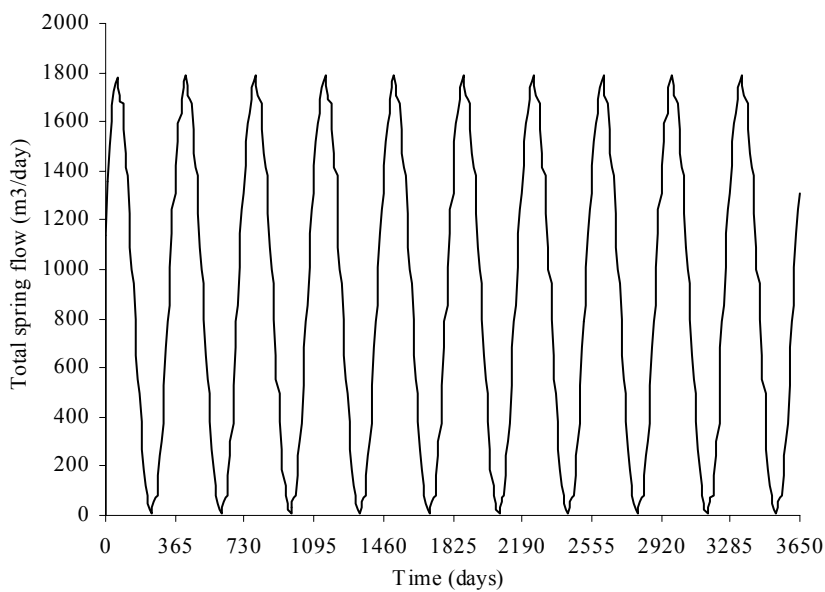


Figure 22 Simulated spring flows in the unconfined sloping bed model

6 Anisotropy

6.1 THE VALIDATION TEST PROBLEM

Horizontal anisotropy is incorporated in ZOOMQ3D. Hydraulic conductivity can be specified at each model node in both the x and y-directions. The inclusion of anisotropy in ZOOMQ3D is tested through comparison with an analytical solution and a MODFLOW model presented by Anderson (1993). Anisotropic aquifers are simulated using both uniform and locally refined grids.

Anderson (1993) presents an analytical solution to an example anisotropic aquifer problem, which is also modelled using MODFLOW. The model consists of an effectively infinite horizontal confined aquifer from which a well abstracts water at a constant rate. The aquifer is ten times as transmissive in the x-direction as in the y-direction. The groundwater head profile is initially flat and the drawdown is monitored at three points: 55 m from the pumping well in both the x and y-directions and at 77.8 m from the well along a direction 45 degrees from the co-ordinate axes. The model parameters are listed in Table 8.

Table 8 Model parameters for anisotropic aquifer test problem

Initial head	0 m
Transmissivity, T_{xx}	198.72 m ² /day
Transmissivity, T_{yy}	19.872 m ² /day
Storage coefficient	0.00075
Pumping rate	345.6 m ³ /day

The aquifer is simulated using ZOOMQ3D based on a number of different model meshes. Each model is discussed in the following subsections. First, the MODFLOW model grid is described.

6.2 THE MODFLOW MODEL

The grid spacing of the MODFLOW model of Anderson (1993) is defined in Table 9. Grid spacing is the same in the x and y-directions. The pumping well is located at the centre of the model, which is 2 km square. The observation wells located parallel to the co-ordinate axes are two blocks from the central model block.

Table 9 Grid spacing of MODFLOW model of anisotropic aquifer

Column/row number	Block width/length	Column/row number	Block width/length
1	300	11	30
2	200	12	30
3	150	13	40
4	100	14	60
5	80	15	80
6	60	16	100
7	40	17	150
8	30	18	200
9	30	19	300
10	20		

6.3 ZOOMQ3D MODEL 1 – REGULAR 27.5 M MESH MODEL

The comparisons between the analytical solution, MODFLOW model and this ZOOMQ3D model based on a regular 27.5 m square mesh are shown in Figure 23. The three graphs show the drawdown monitored at the three observation wells over time. These are in good agreement.

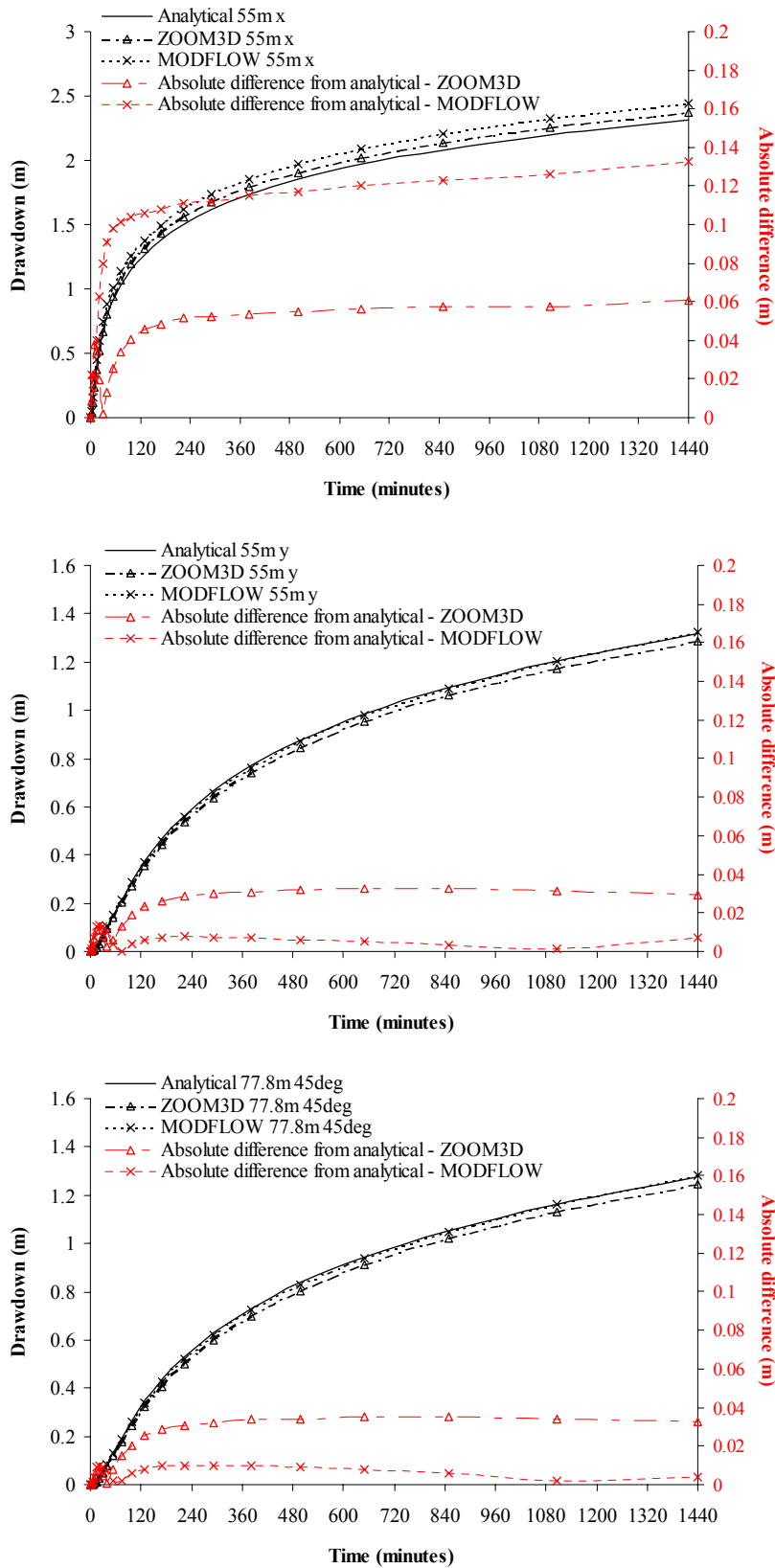
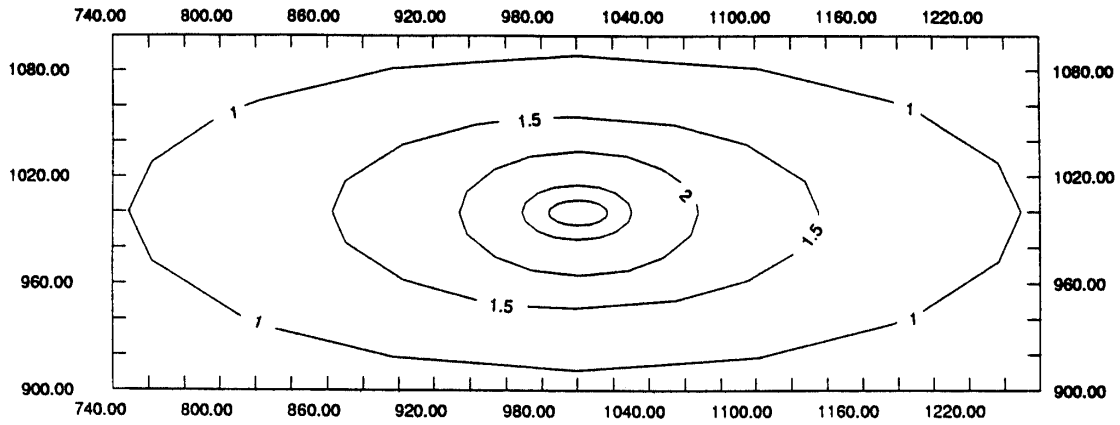
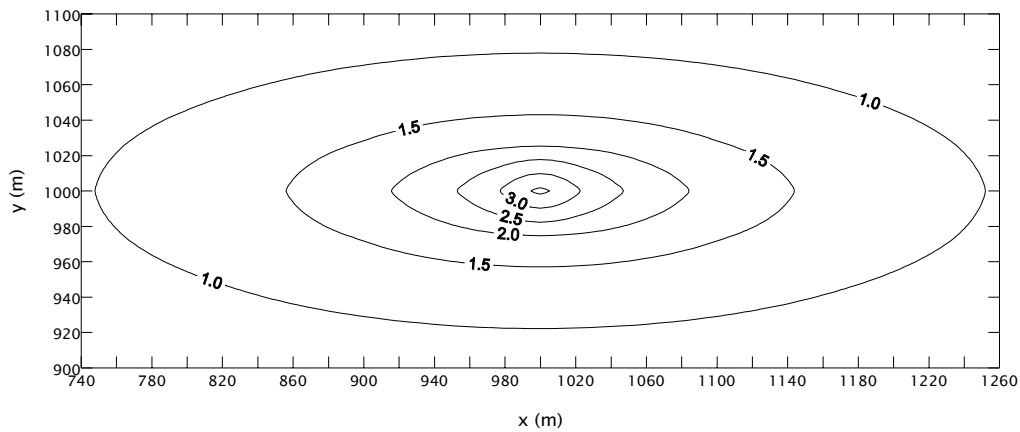


Figure 23 Comparison of 27.5 m square mesh ZOOMQ3D model with analytical solution and MODFLOW model

Anderson (1993) plots the groundwater heads contours at the end of the one-day pumping test. These are shown in Figure 24a. The groundwater contours simulated by ZOOMQ3D at the end of the one-day pumping test are plotted in Figure 24b. It is difficult to distinguish differences between the two contours plots, though the Anderson (1993) model results in a slightly larger cone of depression in the y-direction.



a)



b)

Figure 24 Groundwater head contours at the end of the one-day pumping test simulated by a) the MODFLOW model of Anderson (1993) and b) ZOOMQ3D

6.4 ZOOMQ3D MODEL 2 – LOCALLY REFINED MESH

The locally refined mesh model is shown in Figure 25. The model is 2 km and is composed of a coarse base mesh 55 m square. The grid is refined in two steps, first to 27.5 m square cells and then to 6.875 m square cells. The comparison between the ZOOMQ3D and MODFLOW models and the analytical solution is shown in Figure 26. The ZOOMQ3D model is again in close agreement with the analytical solution indicating that the use of the local grid refinement technique is valid in anisotropic aquifers. Further investigation is required to ascertain why ZOOMQ3D is significantly more accurate than MODFLOW in the x-direction but similar to MODFLOW in the y-direction.

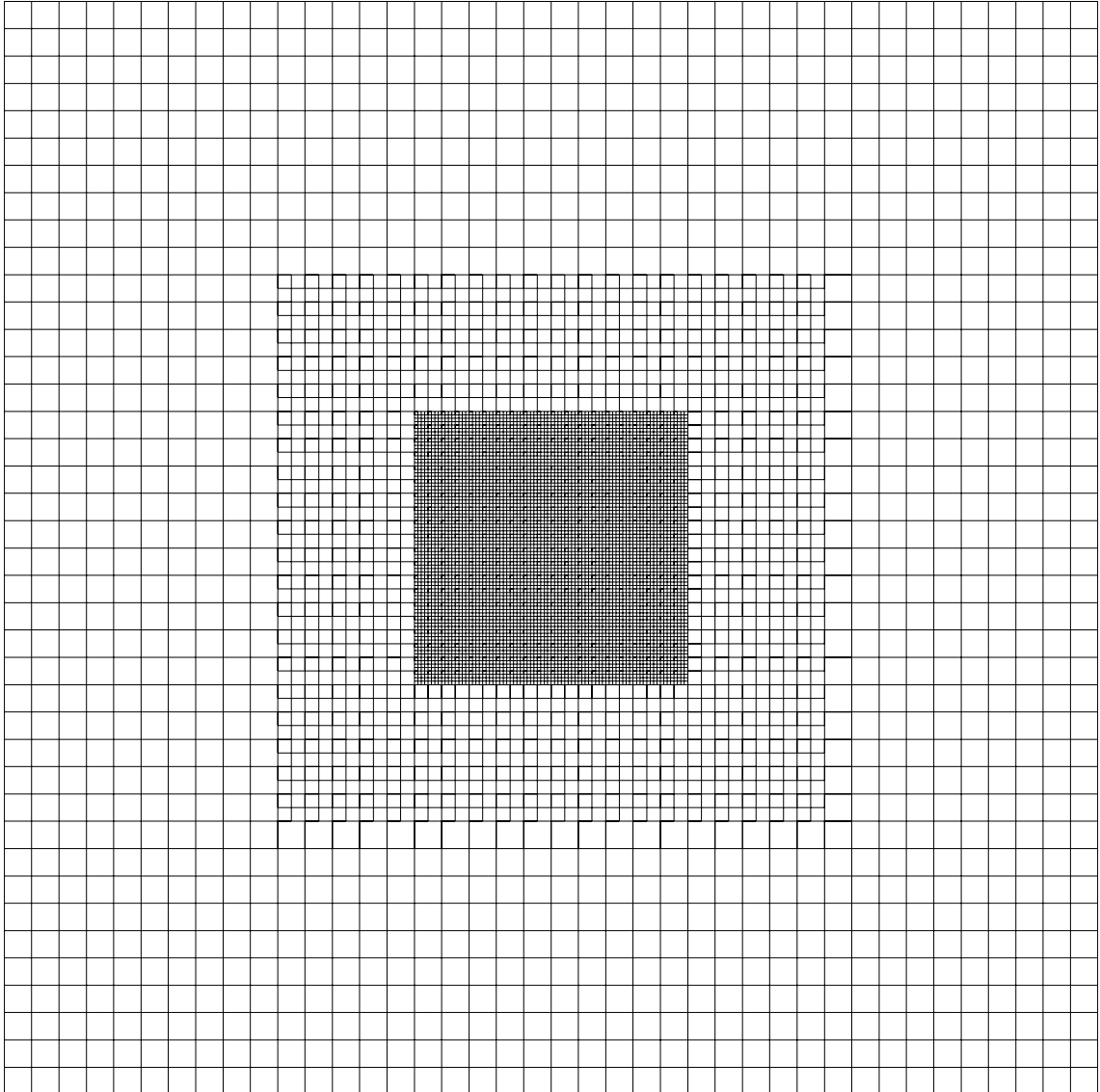


Figure 25 Locally refined grid ZOOMQ3D Model 2 to simulate anisotropic aquifer

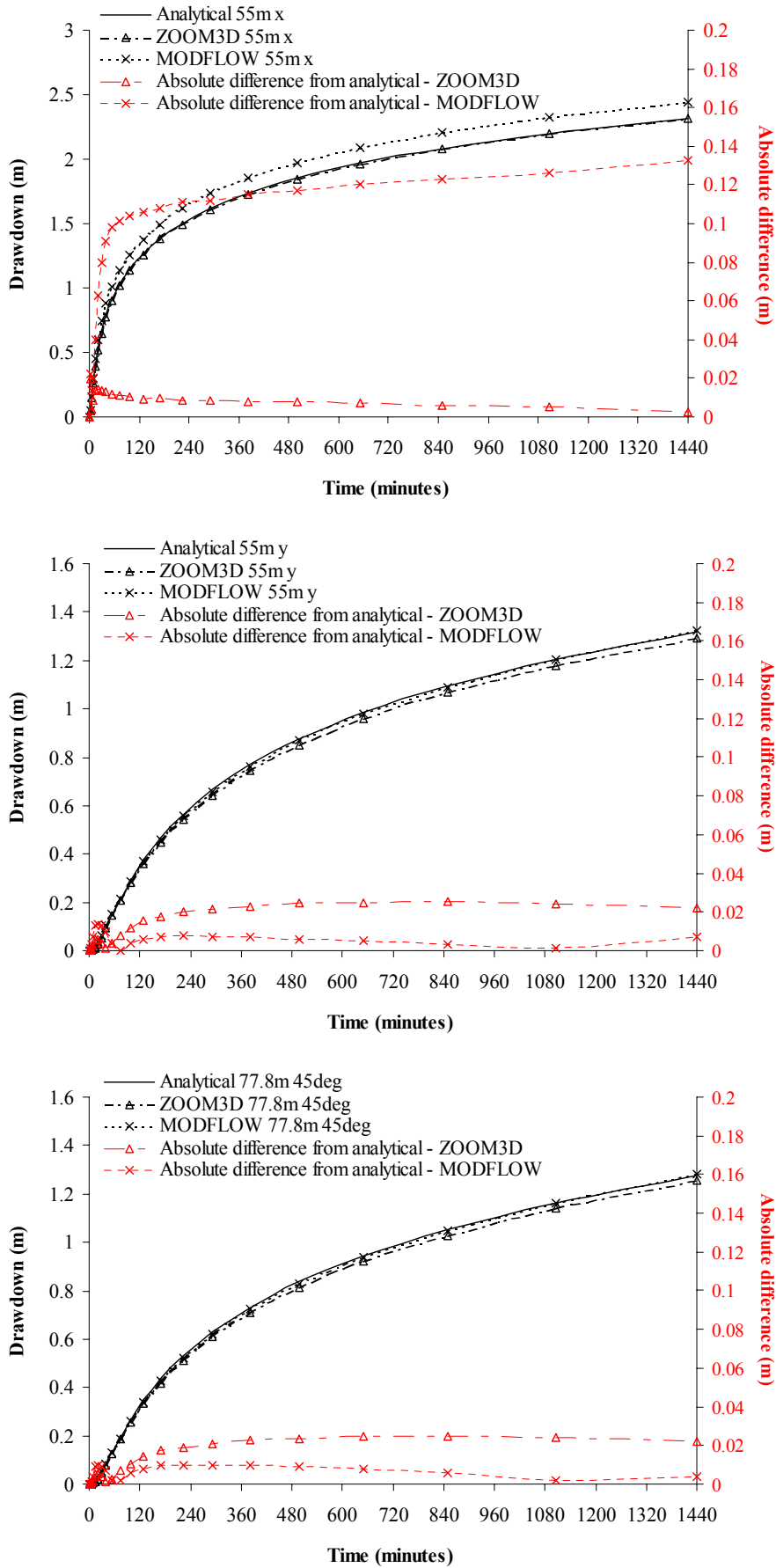


Figure 26 Comparison of refined grid ZOOMQ3D model with analytical solution and MODFLOW model

6.5 ZOOMQ3D MODEL 3 – LOCALLY REFINED MESH

The locally refined mesh model shown in Figure 27 was constructed by accident and used to simulate the anisotropic aquifer. It is the same as the model described in the previous section except for the fact that the south-west corners of the refined grids coincide. Consequently, the refinement rule stating that a grid should not be refined a more than a factor of five is broken. The mesh spacing reduces from 55 m to 6.875 m in one step along the lower left section of the refined grid boundary.

The model could not be made to converge when using this model mesh. In fact, the solution diverged within the SOR iterative solver. However, after moving the finest refined grid towards both the north and east by four mesh intervals of its immediate parent grid, the model converges and is as accurate as the models described above. Also by increasing the finest mesh size to 13.75 m, without moving the positions of the grids, the model also converged to the analytical solution.

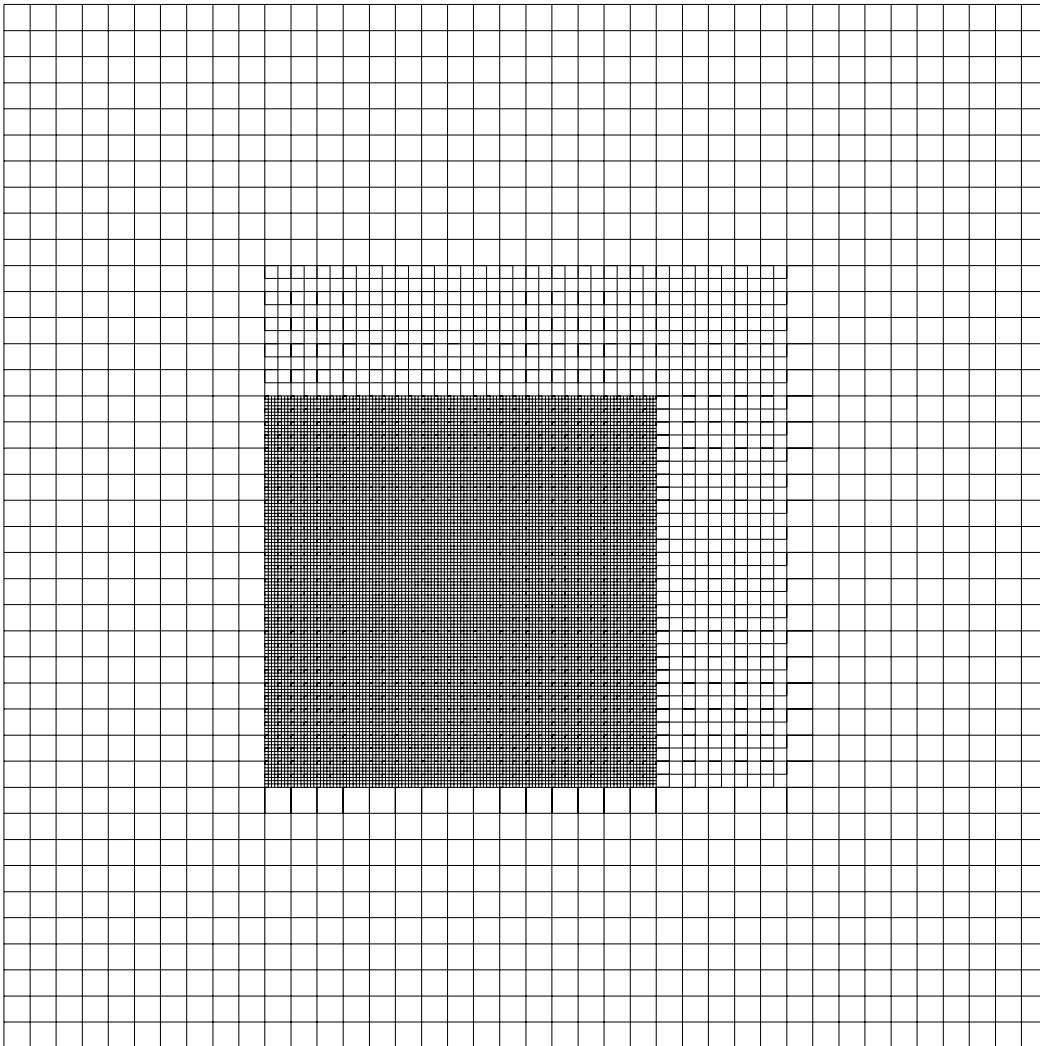


Figure 27 Locally refined grid ZOOMQ3D Model 3 to simulate anisotropic aquifer

7 Numerical solvers

Currently only one numerical solution algorithm is used in ZOOMQ3D to solve the finite difference equations. This is the *successive over-relaxation* method, which is a simple to code but robust algorithm. ZOOMQ3D's code has been updated to allow the rapid construction and implementation of other numerical solution algorithms. The SOR algorithm has been encapsulated in a CSORSolver class. This class is derived from the base class CSolver. A single parameter is passed into the one CSORSolver object created during a model run: a pointer to the top layer of the model. The CSORSolver object then extracts the information from the nodes of the various layers and their grids in order to solve the equations.

New solution methods are now more easily incorporated in ZOOMQ3D because individual bespoke solver objects can be written which encapsulate a solution technique. The incorporation of solution methods to the model is made simple because of the use of *inheritance*. For example, a new class could be written to encapsulate an alternating-direction implicit (ADI) method to solve the groundwater flow equations. This class would derive the data and functionality of the base class CSolver. Again its interface would consist of one member function, which would receive and store a pointer to the top layer of the model. Through this one pointer the created ADI solver object would have access (through the member functions of the objects in the layer-base grid-subgrid-node hierarchy) to the parameter values required to solve the system of partial differential equations.

8 The simulation of ephemeral rivers

8.1 BACKGROUND

The earlier model, ZOOM2D, simulates rivers adequately in most situations but can produce flow balance errors when simulating ephemeral rivers. This is because 'magic' water is created when river nodes dry. Leakage from the river is represented by a linear mechanism based on the difference in head between the aquifer and the river. This is an implicit mechanism because the groundwater head at the end of the time step is used to calculate river leakage. Nodal river flows are also calculated at the end of the time step within an accounting procedure. Flow accounting starts at the nodes at the upstream ends of the river branches. Along a losing stretch nodal river flows decrease downstream. A node may be reached where the flow arriving from upstream is insufficient to satisfy leakage to the aquifer. The river then becomes dry and water is created. That is, more water leaks from the river node than arrives from upstream. Recall that the leakage rate depends on the groundwater head computed at the end of the time step. Because the flow arriving to a node from upstream is not calculated until the end of the time step, it is not possible to determine at the start of a time step if 'magic' water will be created. Consequently, it is difficult to limit the leakage from the river at the start of the time step to the flow in the river. This is because the flow in the river is unknown until the finite difference equations have been solved and the river leakage has been computed using the new groundwater heads.

This problem has been solved in ZOOMQ3D using a cyclical process. If, at the end of a time step, it is found that magic water is created, the time step is repeated. Leakage from drying river nodes is limited to the flow arriving at the node. This upstream flow is calculated during the flow accounting procedure at the end of the time step. The finite difference equations are re-solved using the newly specified leakage rates at the drying nodes. However, specifying the leakage rates causes the solution to change, which in turn affects the flows in the river and the

amount that can be allowed to leak from the drying nodes. Consequently, more than two cycles may be required to identify a solution.

Two tests have been performed to ensure the correct operation of the cyclical process when river nodes dry up. These are described in the next two sections. In addition, the modified model is validated again against the analytical solution presented by Oakes and Wilkinson (1972), which is described by Prudic (1989). This is a solution to the discharge in a perennially flowing river and the groundwater head nearby.

8.2 THE INFLUENCE OF GROUNDWATER ABSTRACTION ON RIVER FLOW

A ZOOMQ3D model is constructed to examine the drying and re-wetting of rivers. The river leakage mechanism is validated by examining the behaviour of river flows and groundwater heads and by checking that nodal and global flow imbalances are negligible. The model is 10 km square and has impermeable boundaries on all sides. The aquifer has a constant uniform transmissivity of $100 \text{ m}^2/\text{day}$ and storage coefficient of 10^{-4} and receives recharge at a rate of $0.1 \text{ mm}/\text{day}$ over its whole area. A river runs through the centre of the aquifer from the north to the south. The flow at its upstream end is specified to be $4700 \text{ m}^3/\text{day}$. The river stage and river bed elevation are constant along the full length of the river and are 100 m and 99 m above the base of the aquifer, or datum, respectively. The river is 10 m wide and has a bed thickness of 1 m. The vertical hydraulic conductivity of the river bed is $0.1 \text{ m}/\text{d}$. A pumped well is located at (5000 m, 7000 m) taking the origin as the lower left hand corner of the model domain.

A steady state solution is computed based on a constant abstraction rate of 10 ML/d from the well. This pumping rate does not cause the river to dry at any point. The steady-state groundwater heads and river flows are used as initial conditions for a time-variant run simulating a 10-year period. For the first four years of the simulation the abstraction rate is 14.2 ML/d, which is sufficient to dry the river. The pumping rate is reduced to 10 ML/d for the final six-year period, during which time the dry sections of the river begin to flow again as the initial steady state conditions are approached.

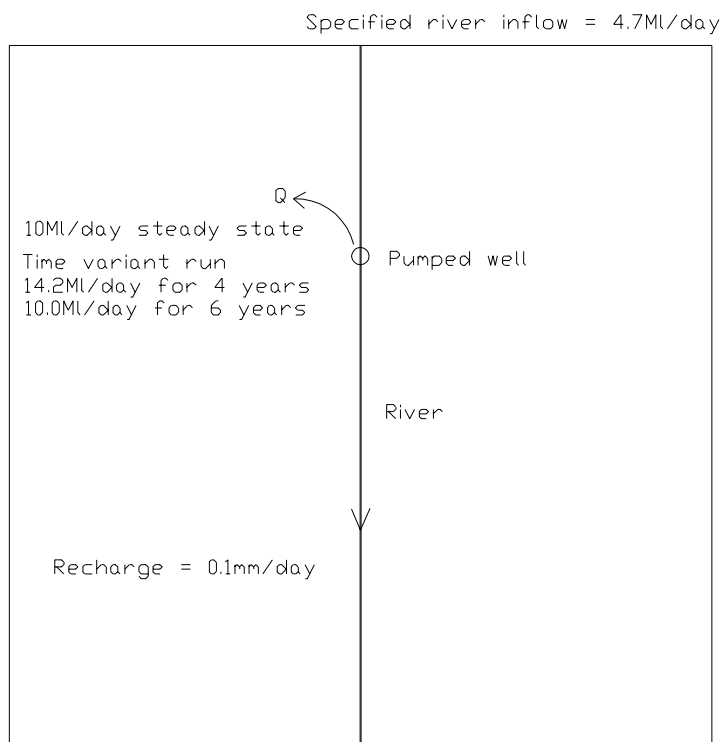


Figure 28 Model configuration for river/groundwater abstraction test problem

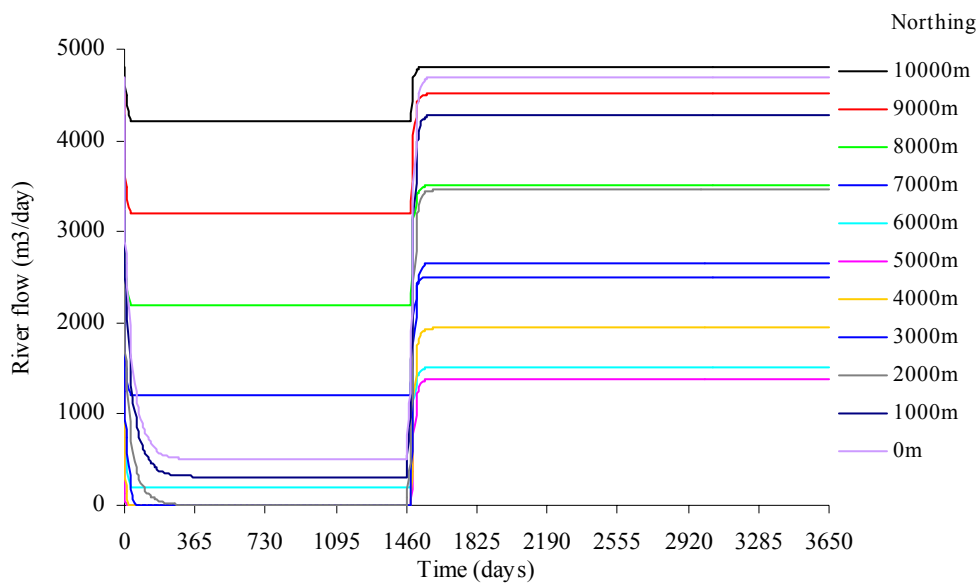


Figure 29 Nodal river flow hydrographs

Groundwater heads beneath the river are monitored during the simulation, as is the flow at each river node. These are plotted in Figure 29 and Figure 30, respectively. The river flows and groundwater heads vary as expected in response to the changes in groundwater abstraction. Global and nodal flow imbalances are monitored throughout the simulation. Nodal flow imbalances are less than the user defined convergence criterion of $5 \times 10^{-10} \text{ m}^3/\text{day}$. The global flow imbalance is approximately an order of magnitude greater, but is still extremely small.

Groundwater heads beneath the river and nodal river flows are listed in Table 10 at the start and after four years of the simulation. The river flows can be used to calculate a global flow balance. At $t = 4$ years (1460-days) total recharge is 10 MI/d, abstraction is 14.2 MI/d and specified river inflow is 4.7 MI/d. Summing these inflows and outflows gives 0.5 MI/d, which is equivalent to the river flow at its downstream end. Therefore, the model maintains a global flow balance.

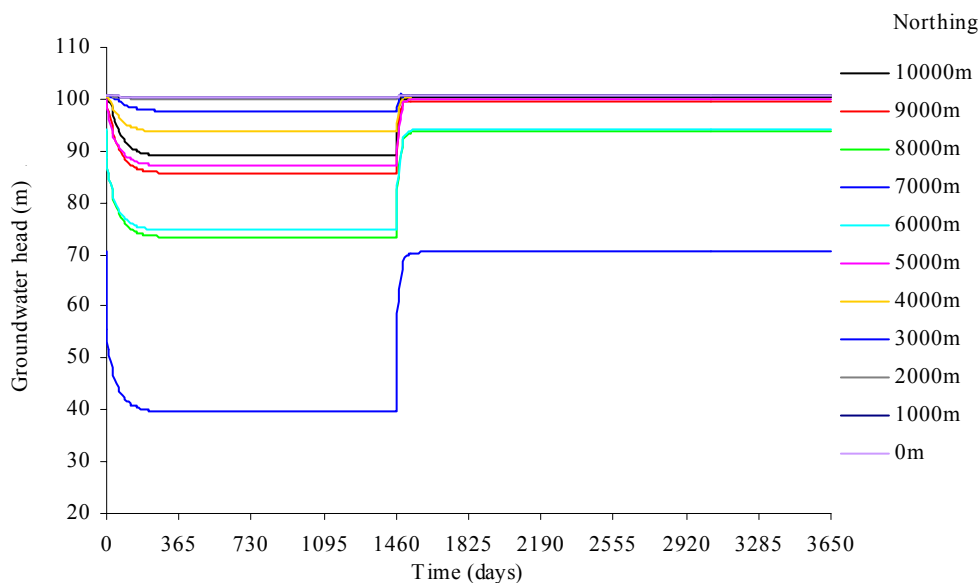


Figure 30 Observed groundwater heads at nodes beneath river

Table 10 Nodal river flows and groundwater heads beneath the river

Northing (m)	River flow (m ³ /day)		Groundwater head (m)	
	t = 0	t = 4 years	t = 0	t = 4 years
10000	4808.3	4200	100.2	89.0
9000	4510.2	3200	99.7	85.7
8000	3510.2	2200	93.7	73.3
7000	2510.2	1200	70.4	39.5
6000	1510.2	200	94.0	74.6
5000	1389.6	0	99.8	87.1
4000	1943.1	0	100.5	93.6
3000	2663.9	0	100.7	97.7
2000	3456.2	2.1	100.7	100.0
1000	4282.0	314.3	100.8	100.3
0	4700	500	100.8	100.3

8.3 SLOPING RIVER MODEL WITH SINUSOIDALLY VARYING RECHARGE

The test is based on a model similar to that used in Section 8.2. The model is 10 km square and has impermeable boundaries on all sides. The aquifer has a constant uniform transmissivity of 100 m²/day and storage coefficient of 10⁻⁴. A river runs through the centre of the aquifer from the north to the south. In this model, no flow enters at the model at its upstream end. Also, the river stage and bed elevation vary linearly from north to south. At its upstream end the river stage and bed elevation are 150 m and 149 m above the base of the aquifer, respectively and at its downstream end they are 100 m and 99 m above the base of the aquifer. The base of the aquifer is taken as the datum. The river is 10 m wide and has a bed thickness of 1 m. The vertical hydraulic conductivity of the river bed is 0.1 m/d. Recharge is uniformly distributed over the whole aquifer but varies sinusoidally in time with a period of one-year. The monthly recharge rates are listed in Table 11.

Table 11 Monthly recharge rates for model of sloping river

Month	Recharge (mm/d)	Month	Recharge (mm/d)
1	0.5	7	0.0
2	0.5	8	0.0
3	0.4	9	0.1
4	0.3	10	0.2
5	0.2	11	0.3
6	0.1	12	0.4

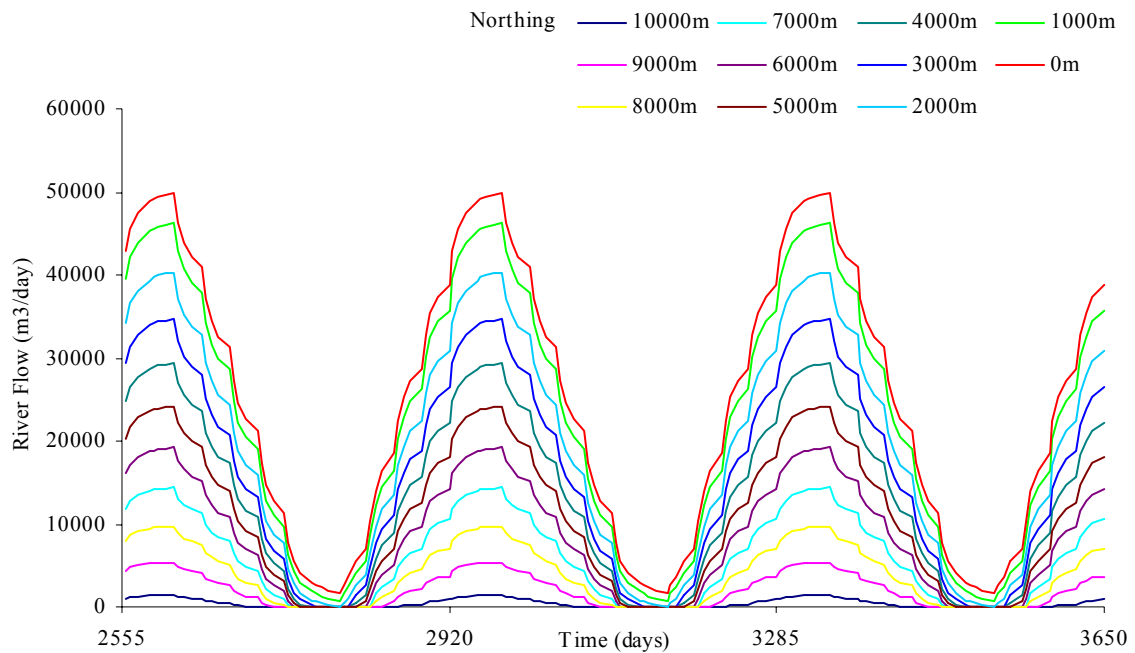


Figure 31 Simulated river flows in sloping bed aquifer at dynamic balance

The model simulates a 10-year period. Initially, all groundwater heads are 100 m above datum and the river flow is 1 Ml/d along its full length. Figure 31 shows the simulated river flows at each node of the river over the final three years of the simulation. These indicate that the model has reached a state of dynamic balance and that the model is operating as expected. Upstream of northing 2000 m the river de-waters during the summer months. The figure indicates that the headwater of the river migrates up and downstream during the year. The river flows are highest at the end of February and lowest at the end of August. These are listed in Table 12.

Nodal and global flow balances are observed during the simulation. Nodal flow imbalances are less than the convergence criterion of $5 \times 10^{-10} \text{ m}^3/\text{day}$. Global flow imbalances at each time step are approximately one order of magnitude greater but still negligible. Consequently, it is concluded that water is not being created as river nodes dry.

Table 12 High and low river flows in sloping river at dynamic balance

Northing (m)	River flow (m^3/day)	
	End of February	End of August
10000	1408.2	0
9000	5382.9	0
8000	9756.8	0
7000	14379.1	0
6000	19192.9	0
5000	24175.6	0
4000	29327.1	0
3000	34670.1	0
2000	40261.6	26.0
1000	46252.2	701.7
0	49826.7	1639.5

8.4 OAKES AND WILKINSON ANALYTICAL SOLUTION TO TIME VARIANT FLOW IN A PERENNIAL RIVER

The two previous tests of the river-aquifer interaction mechanism indicate that it operates correctly when simulating ephemeral rivers. However, they are based purely on the examination of flow balances and the visual inspection of groundwater head and river flow. A more rigorous test is performed in this example using an analytical solution to a time-variant river-aquifer interaction problem presented by Oakes and Wilkinson (1972). The following test is based on the work of Prudic (1989) who uses the analytical solution to validate MODFLOW's (McDonald and Harbaugh, 1988) stream flow package. Consequently, all data for the test is taken from Prudic's investigation.

The ZOOMQ3D model constructed in this test is based on the MODFLOW model of Prudic (1989). This is shown in Figure 32. The MODFLOW model is 8000 ft from east to west and 13000 ft from north to south. The sizes of the model blocks are shown in the figure. The aquifer is homogeneous and has a transmissivity of 3200 ft²/day and a storage coefficient of 0.2. The river runs in a straight line through the centre of the model from north to south. It is assumed to fully penetrate the aquifer and to be in direct contact with the aquifer. This assumption is incorporated by specifying a large river bed conductance, which is equivalent to the transmissivity of the aquifer divided by an assumed 1 ft river bed thickness. This gives a river bed conductance of 3,200 ft/d. The length of each river reach is 1000 ft and the width of the river is assumed to be equal to the depth of the aquifer though a precise value is not given by Prudic (1989). Though the river effectively acts as a line of fixed head nodes it is included in the model to test whether the stream package correctly accumulates the flow from the aquifer to the river.

Annual recharge totals 1.5 ft and is applied uniformly over the aquifer. However, the daily recharge rate varies sinusoidally over the first 180-days of the 360-day recharge cycle as shown in Figure 33. No recharge occurs over the second 180-day period. The sinusoidal recharge pattern is divided into twelve fifteen-day periods over each of which the mid-interval recharge rate is applied. These recharge rates are calculated directly from Figure 33 and are listed in Table 13.

Table 13 Daily recharge rates calculated from Figure 33

Period	Recharge rate (hundredths of a foot per day)
0 – 15 days	0.0386
15 – 30 days	0.2460
30 – 45 days	0.6113
45 – 60 days	1.0226
60 – 75 days	1.4334
75 – 90 days	1.6480
90 – 105 days	1.6480
105 – 120 days	1.4334
120 – 135 days	1.0226
135 – 150 days	0.6113
150 – 165 days	0.2460
165 – 180 days	0.0386

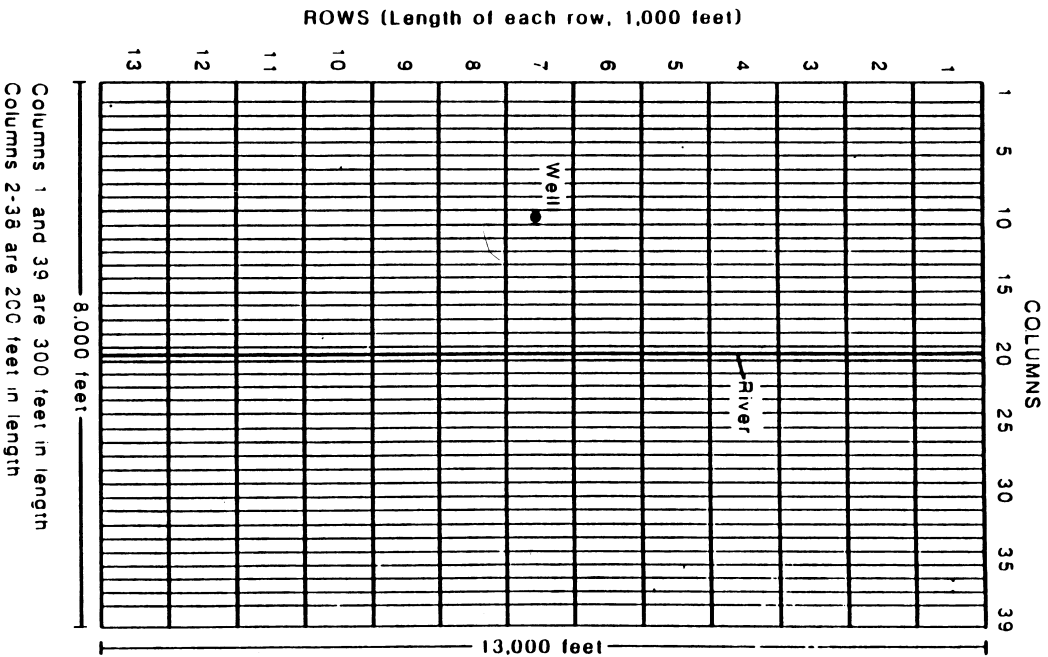


Figure 32 MODFLOW model after Prudic (1989)

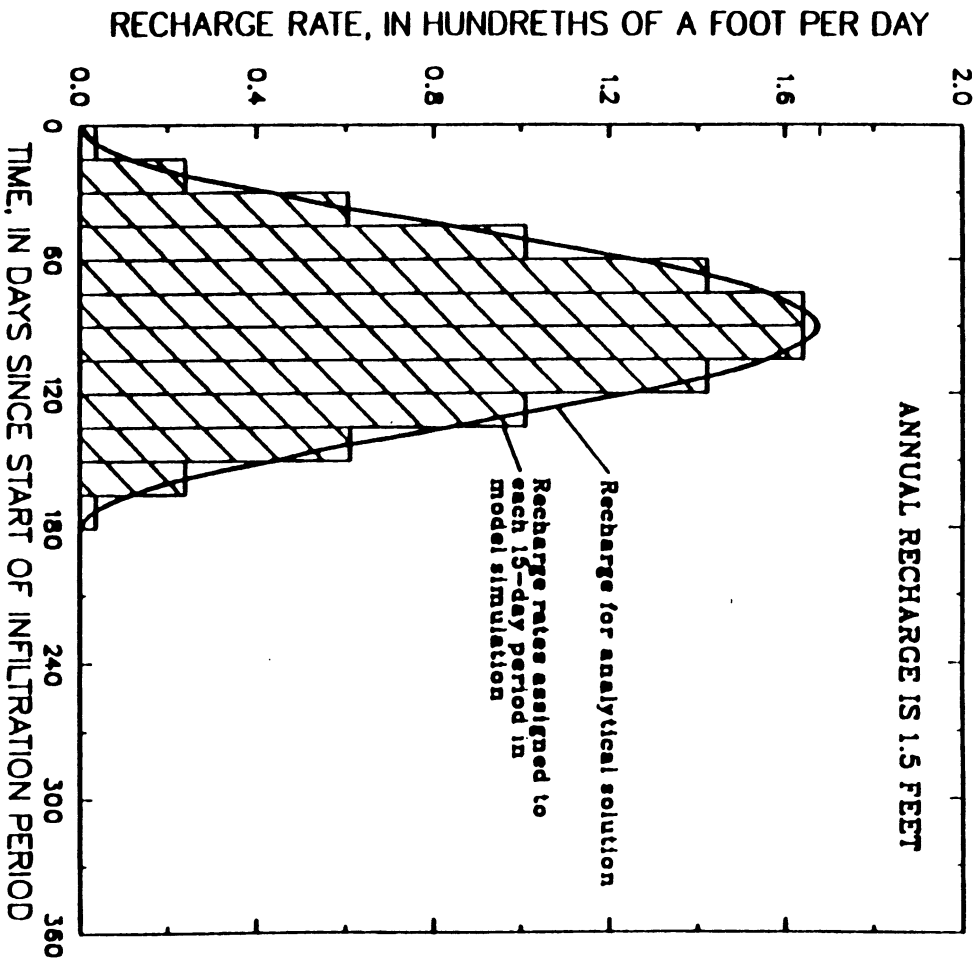


Figure 33 Annual recharge pattern after Prudic (1989)

The model simulates six 360-day periods, the last of which is stated to have reached a stable yearly cycle. The groundwater head in an observation well located at co-ordinate (2000 ft, 6500 ft) from the lower left corner of the model and the downstream flow in the river are recorded over the final 360-day period. Prudic (1989) compares the observed head and river flow at dynamic balance to values given by the analytical solution of Oakes and Wilkinson (1972). The comparisons are shown in Figures 35a and 36a. However, before they are discussed the ZOOMQ3D model constructed for comparison purposes is described. This is shown in Figure 34. The hydraulic parameters of the ZOOMQ3D models are identical to those of the MODFLOW model but the grids differ slightly as ZOOMQ3D is grid-centred and MODFLOW is block-centred. Consequently, the irregular cells at the boundaries of the MODFLOW model do not occur in the ZOOMQ3D models. The ZOOMQ3D model, shown in Figure 34 has a uniform mesh 200 ft by 500 ft in the x and y-directions, respectively. This produces 27 river nodes. Again the model is run to dynamic balance using the same recharge cycle and a 15-day time step. The groundwater head at the observation well shown in red in Figure 34, which is 2000 feet from the river is monitored over the final 360-day period as is the flow in the river at its downstream end. These values are plotted in Figures 35 and 36 along with the data obtained from the MODFLOW model and the analytical solution.

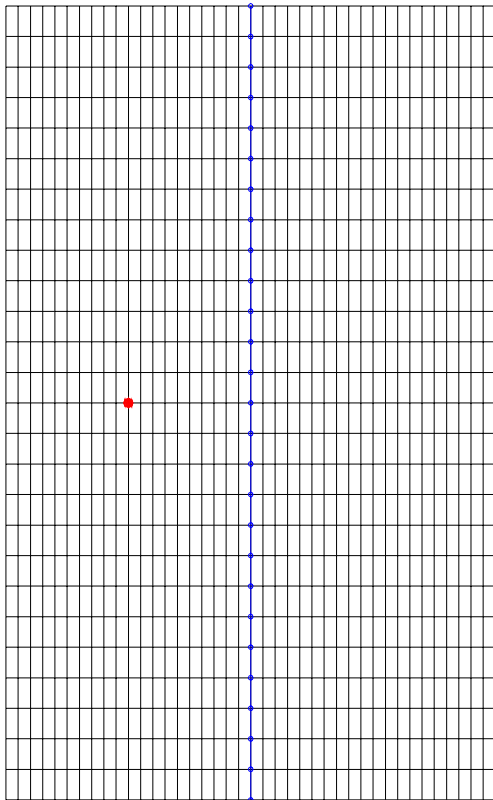
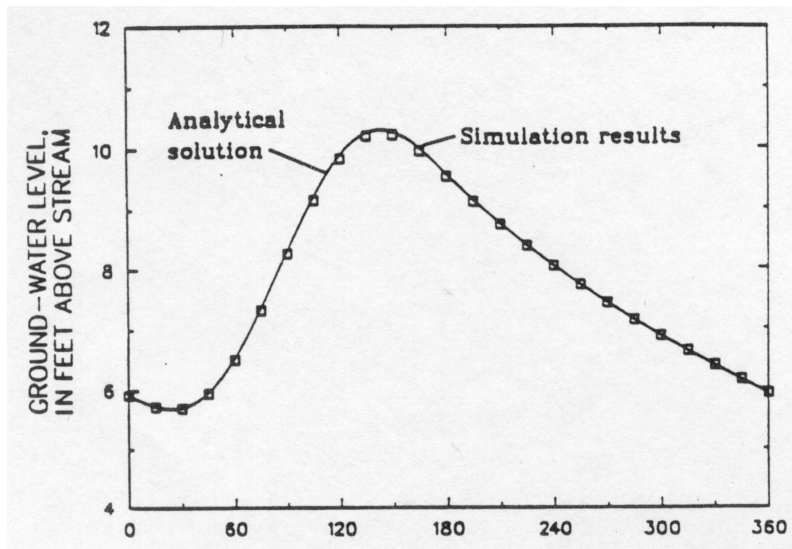
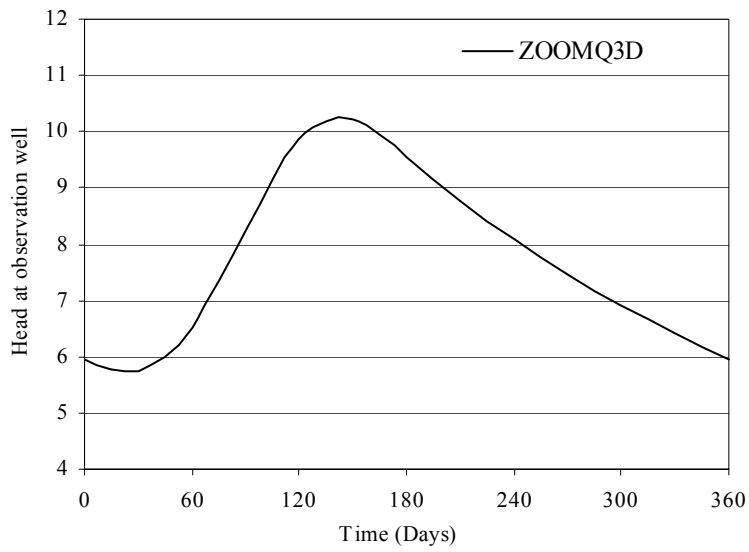


Figure 34 ZOOMQ3D model grid for comparison with the MODFLOW model of Prudic (1989) and the analytical solution of Oakes and Wilkinson (1972)

In Figures 35a and b the groundwater head at the observation well is plotted for the analytical solution, the MODFLOW model and the ZOOMQ3D models over a complete 360-day period at dynamic balance. These show good agreement. The flow at the downstream end of the river computed in the analytical solution and the two models, shown in Figures 36a and b, also agree well. These figures illustrate that the river-aquifer interaction mechanism included in ZOOMQ3D is accurate and comparable to the MODFLOW stream package.

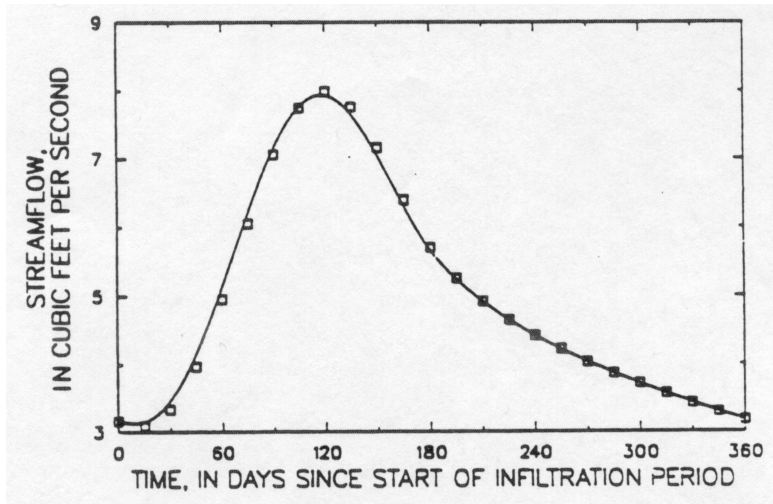


a)

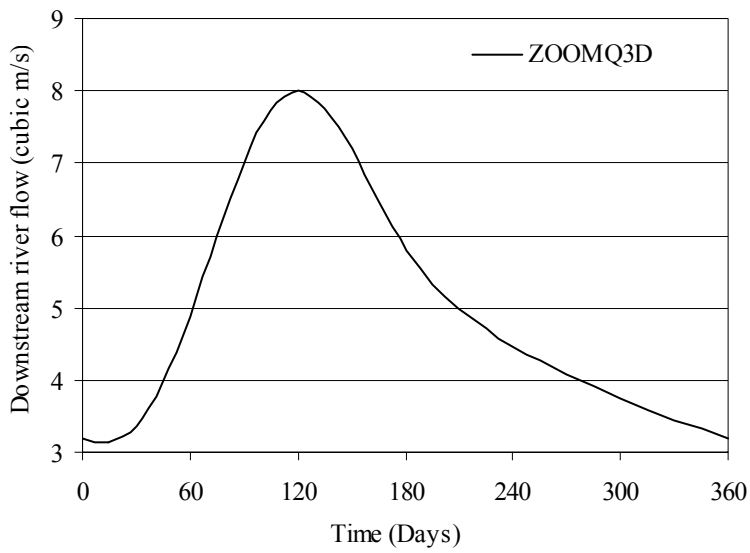


b)

Figure 35 Computed head at the observation well by the a) the MODFLOW model of Prudic (1989) and the analytical solution b) the ZOOMQ3D model



a)



b)

Figure 36 Computed downstream river flow by the a) the MODFLOW model of Prudic (1989) and the analytical solution b) the ZOOMQ3D model

9 Concluding remarks

This report has described the further development of the object-oriented regional groundwater model developed by The University of Birmingham (2001). A number of additional mechanisms have been introduced to satisfy generally accepted functional requirements of a commonly applied regional groundwater flow model. The modified model, ZOOMQ3D, has been validated through comparison with analytical solutions and with models described in groundwater flow modelling literature.

The representation of layers and the mechanisms by which nodes can desaturate, de-water and re-wet are similar to those incorporated in MODFLOW (McDonald and Harbaugh, 1988). Unconfined aquifers are simulated by defining transmissivity to be a function of saturated thickness. In MODFLOW, transmissivity is updated during each iteration of the solution algorithm, for example during the iterations of the successive over-relaxation (SOR) solution method. However, this means that the coefficients in the formulation of the finite difference equations change during the solution process. That is, the equations change whilst their solution is being sought. Whilst in practice this technique is usually found to be satisfactory, a different approach is adopted here in which the coefficients in the system of simultaneous equations do not change during the solution process. Instead, a *cyclical* procedure is adopted in which the solution for the current time step is repeatedly calculated. Transmissivity is updated after the solution for the current time step is calculated and not at the end of each iteration. The solution for the current time step is then recalculated using the new values of transmissivity. When the change in transmissivity between time step repetitions, or cycles, is less than a user-defined value the simulation progresses to the next time step. The comparative advantages and disadvantages of the two approaches will be determined through application of the model. Whilst it is thought that MODFLOW may converge more rapidly in some situations, the approach adopted in ZOOMQ3D is likely to be more stable.

The de-watering and re-wetting of model nodes must be implemented with care in a numerical model. The approach applied in ZOOMQ3D is identical to that applied in MODFLOW. However, the management is significantly simplified in ZOOMQ3D because of the use of objects. A node de-waters when the groundwater head falls below the elevation of its base. Care must then be taken to ensure that recharge is applied to the node underneath, otherwise water will be lost within the model. In ZOOMQ3D, the management of this change in the application of recharge requires a single operation. A pointer from the CInteractionNode object, the object which 'passes' recharge to the node, just has to be switched to the lower node. River-aquifer interaction is also 'directed' through CInteractionNodes and thus this one modification also means that river leakage is always based on the head in the upper most active layer. This is one example of the benefits of the encapsulation of functionality in objects, and the use of pointers. The coding of such changes in models written in procedural languages is, generally, significantly more complicated.

Springs are usually simulated in models using a head dependent leakage mechanism. This mechanism was already incorporated in the model. However, the conceptualisation of a spring in this way, in which the outflow from the aquifer is based on a 'bed conductance' could be argued to be simplistic. Consequently, another spring mechanism has been developed in which spring flows are dependent on the groundwater head in the aquifer, and not governed by a conductance term. Instead, spring flows can only be adjusted by modifying the transmissivity of the aquifer in the region of the spring. Consequently, the general pattern of flow within the aquifer determines the outflow at a spring location. The potential benefit of this mechanism is unknown at this stage but should be determined through the application of the model.

As stated in the introduction, one of the aims of this development work is to provide the modelling community with a model with which to assess the benefits of the object-oriented approach to groundwater modelling. Consequently the objective is to produce a model, which satisfies generally-accepted functional requirements of a commonly-applied regional groundwater flow model. The work reported here means that this aim is almost achieved, however some further additions to the model are required to fulfil this objective. The major outstanding task is to incorporate the ability to track particles through the model under both steady state and time variant conditions.

With particular regard to UK hydrogeology, another requirement of a regional groundwater model may be the incorporation of variations in hydraulic conductivity with depth. This has recently been implemented in MODFLOW by the Environment Agency (Environment Agency, 1999) and thus to represent the hydraulic behaviour of a Chalk aquifer it should be incorporated into ZOOMQ3D.

Finally, the current model only incorporates one method to solve the system of finite difference equation; *successive over-relaxation* (SOR). However, the object-oriented approach means that new solution methods can be written easily and rapidly if so required.

Once these additional components have been included it should be the intention of the project partners to disseminate the code and the philosophy behind it to as many modellers within their organisations as possible. This should generate valuable feedback that will be of assistance in the further development of the final object-oriented regional groundwater model that better represents UK hydrogeology.

10 References

- ANDERSON P.F. (1993). A manual of instructional problems for the USGS MODFLOW model. United States Environmental Protection Agency.
- BEAR J. (1979). Hydraulics of groundwater. McGraw-Hill, New York.
- ENVIRONMENT AGENCY. (1999). Representation of the variation of hydraulic conductivity with saturated thickness in MODFLOW. Stage I & II code changes and testing against Birmingham University code. Unpublished report.
- JACKSON C.R. (2000). A novel grid refinement method for regional groundwater flow using object-oriented technology. Ph.D. Thesis, University of Birmingham, Birmingham.
- MCDONALD M.G. and HARBAUGH A.W. (1988). A modular three-dimensional finite-difference ground-water flow model. Techniques of Water Resources Investigations, 06-A1, 576.
- MCDONALD M.G., HARBAUGH A.W., ORR B.R. and ACKERMAN, D.J. (1991). A method for converting no-flow cells to variable-head cells for the U.S. Geological Survey modular finite difference ground-water flow model. U.S. Geological Survey open file report, 91-536.
- OAKES D.B. AND WILKINSON W.B. (1972). Modelling of ground water and surface water systems: I-Theoretical relationships between ground water abstraction and base flow. Water Resources Board, Great Britain, 16, 37.
- PRUDIC D.E. (1989). Documentation of a computer program to simulate stream-aquifer relations using a modular, finite difference, groundwater flow model. US Geological Survey Open File Report, 88-729, 113.
- RUSHTON, K.R. and REDSHAW, S.C. (1979). Seepage and groundwater flow. John Wiley and Sons, Chichester.
- SZEKELY.F. (1998). Windowed spatial zooming in finite-difference ground water flow models. Ground Water, 36, 5, 718-721.
- THE UNIVERSITY OF BIRMINGHAM. (2001). ZOOM2D An object-oriented regional groundwater model incorporating local grid refinement. A user's manual. Unpublished report.